AOPP, UNIVERSITY OF OXFORD

Sloping Convection: An Experimental Investigation in a Baroclinic Annulus With Topography

Second Year DPhil Report

Samuel David Marshall

Lincoln College

Supervisor: Professor Peter Read

30/8/2011

Word Count: 12,530

Abstract

This report documents the second year of work for this thesis, in which a differentially-heated annulus is used to investigate sloping convection. In particular, the investigation will focus on the effects of topography on the atmospheric circulation. To this end a number of experiments were devised, each using a different topographic base to study a different aspect of the impact of topography, motivated by the most notable outstanding questions found in a review of the literature. The experiments would be conducted using an existing apparatus, modified for these studies, the construction and design of which are provided and explained.

First of all, to create a reference point to which all the studies could be compared, it was decided that a control experiment with some simple sinusoidal topography would be employed. This control experiment would also be used to check the readings being obtained against a similar investigation in the literature. For this purpose, the recent studies of Read and Risch (2011) were chosen. This investigation was judged to be successful, finding what was expected to be found, both in terms of a continuation of the readings of Read and Risch, and comparison with the effects of topography found in the literature review. In addition, a sizable number of different flows in terms of characteristics and regimes were observed and documented. Unfortunately, due to various problems with equipment, preliminary observations from the other experiments have yet to be properly carried out. Subsequent years of this thesis will continue these experiments, exploring the effects of blocking via partial barriers, azimuthally differential-heating via thermal topography, and the viability of less-idealised topography via a superposition of wavenumbers. These experiments will be able to compare results with the control study, especially in regard to what regimes are encountered, and where they occur in parameter space.

Table of Contents

Chapter 1

Introduction

Sloping convection – and the accurate comprehension of its implications – are arguably the most important aspects of atmospheric circulation, whether discussing the Earth, other planets within the Solar System, or even exoplanets still to be discovered. Also known as baroclinic instability, sloping convection can occur when a thermally-forced zonal flow causes a shear in the density stratification, as in Figure 1.1.

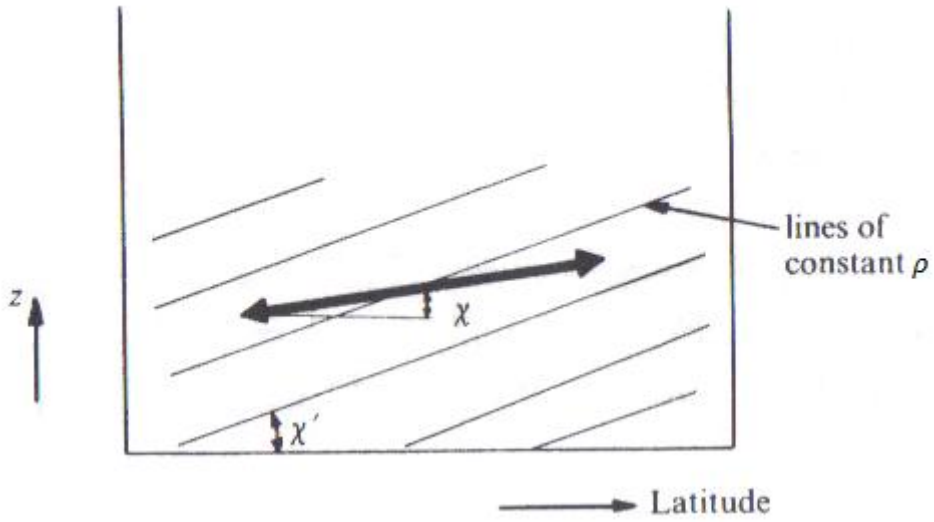

Figure 1.1: Illustration of sloping convection, where χ is the average slope between air parcels in a disturbance and χ' is the slope of the density surfaces [adapted from Houghton (2002)]

If $\chi < \chi'$, this shear leads to an increase in potential energy, due to the interchange of the air parcels between surfaces of different densities. This in turn provides kinetic energy into the system and hence produces instabilities. A more detailed account of this process can be found in Andrews (2000).

The effects of sloping convection on the atmosphere are many and various. For example, Houghton (2002) notes that, outside of the Hadley Cell, sloping convection is the dominant method of heat transport in the atmosphere, and, according to Hide, Lewis and Read (1994), it is also a probable mechanism for the generation of such famous and long-lasting features as the Jovian Great Red Spot.

In the laboratory, sloping convection can be replicated using a piece of equipment known as a differentially-heated rotating annulus. As such, this thesis will utilise this apparatus to study the various impacts that sloping convection of the fluid has on the patterns governing atmospheric circulation, with special focus on the differences between quasi-geostrophic and ageostrophic effects.

1.1 The Annulus

The rotating annulus is the standard for laboratory studies of the atmosphere, especially with topography. Differentially-heated annuli, such as those in Leach (1981), Li, Kung and Pfeffer (1986) and Risch (1999), are cylinders full of fluid on a rotating turntable that contain a second central cylinder which can be cooled, whilst the outer cylinder can be heated – this temperature difference is what drives the flow. In this way, the annulus becomes a simple simulation of the Earth's (or another planet's) atmosphere, as seen from directly above the poles, with the cool middle analogous to the pole, and the heated outer edge analogous to the equator. More specific detail will be provided in a later section.

Annuli have their origin in the early 'dishpan' experiments of the 1800s, most notably that of Vettin (1857), who used a container of ice to cool the center of the fluid. Unfortunately, only Vettin was able to see the importance of this model of the atmosphere, and the development of the experiments stalled. The next time annuli would occur in major literature would be almost one hundred years later, in Hide (1953). Interestingly, these annuli, despite essentially being in their modern form (with only minor differences in materials and structure), were designed to study the thermal convection in the Earth's core. However, Hide did note the possible application to atmospheric circulation. By the time of Hide (1958), interest in atmospheric circulation had overtaken that of the Earth's core and the first modern investigation with an annulus led to the discovery of vacillation and the different flow regimes of the jet stream (including a detailed images of wavenumber-2, wavenumber-3 and wavenumber-4 regimes, described in the next section). Several years later, Hide and Mason (1975) produced the seminal work on annuli, and the basis for most modern experiments. The authors investigated the effects of increasing the rotation rate and thermal forcing on the flow, charting the transition from wavenumber-1, through wavenumber-2, wavenumber-3 and wavenumber-5, up to the chaotic/irregular regimes. As will be seen, the experimental arrangement of this thesis owes a lot to these studies.

1.2 Sloping Convection in the Annulus

The temperature difference of the differentially-heated annulus generates a radial flow (analogous to the atmosphere's meridional flow) that acts to create a baroclinic flow profile. This can be observed by taking temperature readings of the fluid, as illustrated in Figure 1.2, which shows a temperature stratification that represents the sloping density surfaces.

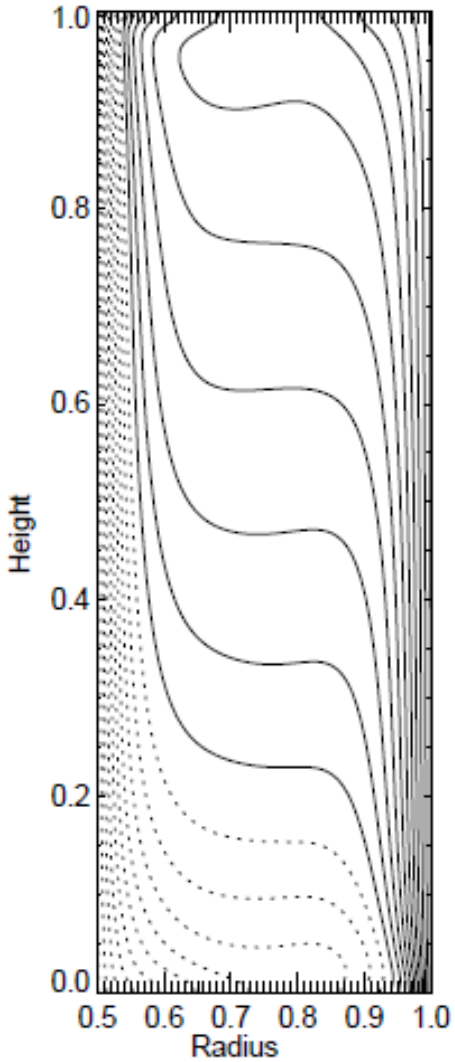

Figure 1.2: Cut-away of computational annulus showing normalised temperature contours with respect to height/depth (y-axis) and radial distance (x-axis), heating occurs at the right-hand wall (x = 1) and cooling occurs at the left-hand wall (x = 0.5) [from Read et al (2004)]

Hence, sloping convection can be simulated in the annulus, along with its dynamical effects on the flow. These effects can be split into two types: quasi-geostrophic and ageostrophic.

The quasi-geostrophic approximation assumes that the Rossby Number (the ratio of inertial acceleration to Coriolis acceleration, explained in the third chapter) is small but non-negligible, allowing derivation of the quasi-geostrophic potential vorticity which, in terms of the streamfunction ψ, can be written in the form:

$$q = f_0 + \beta \cdot y + \frac{d^2\psi}{dx^2} + \frac{d^2\psi}{dy^2} + \frac{d}{dz}\left(\frac{{f_0}^2}{N^2}\frac{d\psi}{dz}\right) \tag{1.1}$$

where x, y and z are the zonal, meridional and vertical directions respectively, β and f_0 (the mean planetary vorticity, which can be omitted due to being constant) are from the beta-plane approximation to the Coriolis parameter, $f \approx f_0 + \beta \cdot y$, and N is the buoyancy frequency. Equation 1.1 is a very useful result, allowing a single unknown, q, to describe the entire motion of the system. As such, quasi-geostrophic models are very common, often employed even when the approximation starts to break down, for instance when topography becomes sufficiently large.

Quasi-geostrophic dynamics are often low-order phenomena, achievable by simple numerical models with only a small number of modes. Ageostrophic dynamics, on the other hand, require either high-resolution computational models or laboratory studies to be observed. In the next two sections, the most important occurrences of both will be briefly introduced and discussed.

1.2.1 Quasi-Geostrophic Dynamics

The most important low-order effect of sloping convection in an annulus is the advent of baroclinic waves. At low rotation rates, flow structure is uniform in the azimuthal direction[1]. Hide and Mason (1975) refer to this region as 'axisymmetric'. When the rotation rate surpasses a certain critical value, however, the flow becomes 'non-axisymmetric' and azimuthal variation is introduced in the form of eddies. The number of eddies that occur increases with increased rotation (and/or thermal forcing) until a second critical value is reached whereupon the structure becomes dominated by chaos. These eddies are baroclinic waves, and are illustrated in Figure 1.3.

[1] Andrews (2000) notes the similarity to the Hadley Cell circulation.

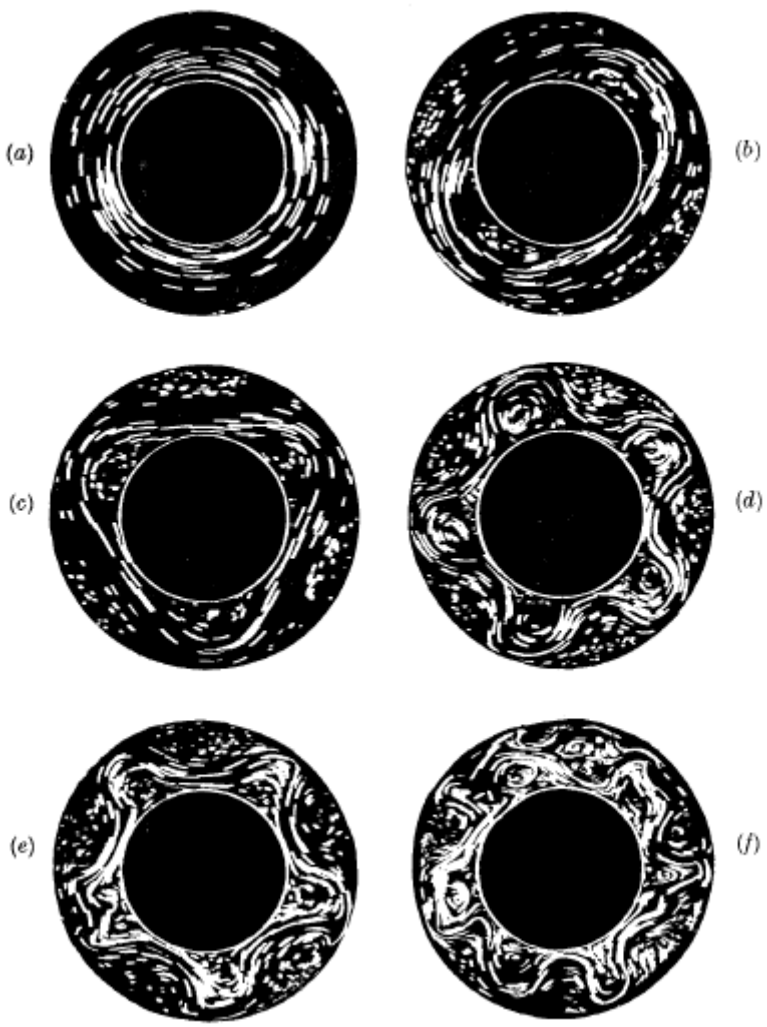

Figure 1.3: Streakline images illustrating how the flow structure develops as rotation rate increases - a.) $\Omega = 0.41$ rads^{-1}, b.) $\Omega = 1.07$ rads^{-1} c.) $\Omega = 1.21$ rads^{-1} d.) $\Omega = 3.22$ rads^{-1} e.) $\Omega = 3.91$ rads^{-1} f.) $\Omega = 6.4$ rads^{-1} [from Hide and Mason (1975)]

Each flow structure is named after the 'period' of the waves, with (b) referred to as wavenumber-2, (c) as wavenumber-3, (d) as wavenumber-5, and so-on. Furthermore, the waves can be either stationary or drifting, depending on whether they oscillate at the same rate as the annulus or not, and either vacillating or steady, depending on whether the eddies maintain a constant size and shape or not. Amplitude vacillation is where the eddies grow or shrink in the radial direction over time, and structural vacillation (which occurs with more intense forcing) is where the eddies change in appearance, for example becoming unevenly spaced around the annulus. These terms will become important in describing the results of this thesis' experiments.

1.2.2 Ageostrophic Dynamics

When topographical features are included in a model, most of the flow dynamics can often be considered to be ageostrophic. This is due to the quasi-geostrophic approximation starting to break down when topography becomes sufficiently large. Benzi et al (1986) stated that, if there were no topography, the long-term atmospheric circulation would be zonally symmetric (although, short-term asymmetry can be caused by differential heating). Hence, topography must have a spatial symmetry-breaking effect, which takes the form of stationary topographic waves, on the zonal flow. These waves[2] are defined as having peaks and troughs that do not move relative to the ground, occurring at locations determined by the shape of the planet's topography. According to Wallace (1983) topographic forcing is dominant at the level of the jetstream, between the middle and upper atmospheres. At sea level, thermal forcing takes over. This is backed up by Held (1983); however he asserts that the effect of topography is still non-negligible at the surface.

Another influence of topography on the atmosphere is the formation of circulation regimes, as explained by Charney and DeVore (1979). Topographical forcing can lead to the development of either a 'low index' flow or a 'high index' flow. The former state (also known as 'blocking') is defined as having "a strong wave component and a weaker zonal component locked close to linear resonance"; this locking is caused by the non-linear interactions of the topography with the zonal flow. The latter state (also known as 'zonal' flow) has "a weak wave component and a stronger zonal component much further from linear resonance". Both states are stable (sometimes also referred to as metastable or quasi-stable), giving rise to the concept of multiple equilibria. Transitions between the two states are forced by baroclinic instabilities of the topographic waves.

As topography is so important to atmospheric circulation (with the above paragraphs only giving a few consequences of its impact), this thesis will take the form of an experimental investigation of topography with regards to the annulus. More impacts of topography will be discussed in Chapter 2, along with unresolved questions found from a review of the literature on the topic. It is the answers to these questions that will determine the course of the topographic study, as well as the precise nature of the experiments to be carried out.

[2] Occasionally referred to as quasi-stationary waves, as in Cehelsky and Tung (1987), for example.

1.3 Summary

The format that this report will take is as follows. Firstly, Chapter 2 will form a literature review of existing topographic studies, describing what unresolved questions about the effects of topography on the atmospheric circulation remain to be investigated, what laboratory work has already been carried out on the subject and how the current apparatus can be altered to investigate these effects. After that, Chapter 3 will be a detailed account of the experimental apparatus that this project will utilise, including the methodology that will be employed and explanations of the experiments to be carried out in the second year of study. The chapter will also contain a short explanation of some of the key dimensionless numbers needed to describe the parameter space. Next, Chapter 4 will provide the results of these experiments, and contain initial observations made. This will be followed by a discussion, Chapter 5, examining the progress of the second year of study and suggesting outstanding issues for later investigation. Chapter 6 will then consolidate all the outstanding issues from these studies in order to create an outline for the aims and objectives for the future progress of the thesis. In addition, a timeline of work until the end of the project will be established and justified. Lastly, a list of the various references used to assemble this report is given.

Chapter 2

Topographic Review

As described in Chapter 1, a major aspect of sloping convection and atmospheric circulation in general is that of topography. As such, this thesis will investigate the effects of topography on the atmospheric circulation using a differentially heated annulus that will be described in Chapter 3. This chapter will therefore give a brief review of the topic, beginning with an assessment of the various unresolved questions found within the literature. Of these problems, the most interesting (and most applicable to the annulus) will be looked at in greater detail, forming an initial outline of the experiments to be carried out in this study.

2.1 Topographic Problems

Within the literature on the topic of topography there are several open questions that have yet to be resolved. In this section, several of the most pressing of these will be studied, looking at the original papers that raised them, any further development in subsequent works, and how the questions could possibly be answered in a thermally-driven annulus.

Possibly the most major question found in the literature is the issue of the existence of multiple equilibria. Most notably, Charney and DeVore (1979), Charney and Straus (1980) and Reinhold and Pierrehumbert (1982) suggested the idea that both the 'low-index' (blocking) and 'high-index' (zonal) regimes (caused by non-linear interactions between the background zonal flow and bottom topography) are meta-stable, meaning both can exist under the same conditions. Transitions between the regimes are caused by barotropic instabilities of the topographic wave and, in turn, cause most of the atmospheric anomalies that are observed.

On the other hand, Tung and Rosenthal (1985) and Cehelsky and Tung (1987) claimed that multiple equilibria are physically possible, but cannot exist in the real atmosphere. They suggested that previous results of multiple equilibria were caused by unrealistic topography or, in the case of Charney, Shukla and Mo (1981) where the topography used is deemed to be sufficiently 'realistic' (illustrated in Figure 2.1), overly-truncated non-linear interactions. In their models, asserted to be better analogies to the atmosphere, no multiple equilibria are found and the regimes are solitary. The

flaw of these papers is that no definition of what is meant by 'realistic' topography is given. Sometimes it appears they are suggesting that topography in previous studies was overly large, but that of Charney, Shukla and Mo (1981) is similar in scale to that of Charney and DeVore (1979). As such, it will be assumed that by 'realistic', they mean a complex topography closer to the distribution of mountains on Earth.

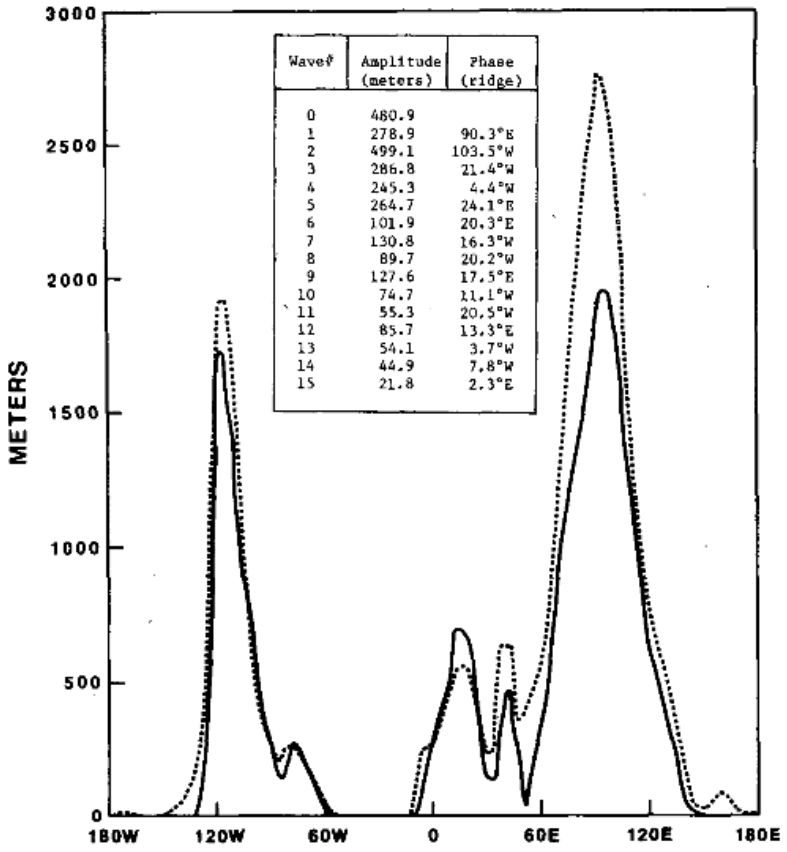

Figure 2.1: 'Realistic' topography, dotted line created from actual topographic measurements [from Charney, Shukla and Mo (1981)]

These papers were in turn rebuffed by Molteni (1996) using high-resolution hemispheric models. Contrary to Tung and Rosenthal (1985) and Cehelsky and Tung (1987), two distinct flow regimes were found, even when a large enough number of degrees of freedom were used to simulate fully non-linear interactions. However, since simple wavenumber-3 topography is employed, it could be argued that multiple equilibria has only been shown to be possible with this type of topography, and furthermore that this model is not 'realistic' enough to be applied to the real atmosphere.

Similarly, Risch (1999) claimed to find laboratory evidence for multiple equilibria in a thermally-forced annulus for both with and without topography. The topography used was a simple wavenumber-2 shape, suggesting that (like in Molteni (1996), above) low-order models that found

multiple equilibria with similar topography were not merely seeing a false positive due to their 'overly-truncated non-linear interactions', as alleged by Tung and Rosenthal (1985) and Cehelsky and Tung (1987). By extension, Risch (1999) notes that this implies that multiple equilibria should also be possible in the baroclinic atmosphere. The need for 'realistic' topography is still an issue, however.

Supporting the other side of the argument, Tian et al (2001)[3] compared similar numerical and laboratory annulus studies, finding stable multiple equilibria to be prevalent in the former, but not to exist at all in the latter. The physical annulus still produced both zonal and blocked regimes, but they were meta-stable, with irregular, sudden transitions. The lack of multiple equilibria could be due to the fact that the annulus is barotropic (forced by jets) as well as the topography being a simple wavenumber-2 type. No transitions were observed in the computational model, possibly due to the lack of three-dimensional effects (this is to be verified via further numerical simulations by Tian).

Recent works, such as Koo and Ghil (2002) and others by the same authors, claim that multiple equilibria can be observed in their models with realistic topography and fully-realised non-linearity. However, the study is, by the authors' own admission, carried out on a low-order model.

In an annulus, though the atmospheric model is simplistic, the non-linear interactions will not be truncated, giving a perfectly 'realistic' flow. Unfortunately, creating 'realistic' topography is more difficult than in a numerical model, especially if fine features are required. If this problem can be overcome, the topography of Charney, Shukla and Mo (1981) can be recreated – with this 'realistic' topography and the fully non-linear interactions of a physical annulus, a definitive investigation into the existence of multiple equilibria could be launched, putting to the test every condition of Tung and Rosenthal (1985) and Cehelsky and Tung (1987) simultaneously.

By going one step further, this could become a new experiment in its own right: carrying out a simple study with basic wavenumber-2 type topography, and then replacing the bottom surface with increasingly more complex mountain distributions (different elevations, asymmetrical locations, multiple peaks of varying height etc) until no further difference between results can be detected. This would give a reasonable definition for a 'realistic' topography and could then be applied to the investigation into multiple equilibria as a future study. Naturally, this experiment would be easier for a computational model, to save having to build many different iterations of the topography, as well as removing the time-consuming task of emptying and refilling the annulus every time each new topography was used. However, the benefits of finding a compromise between realism and manufacturing difficulty could lead to the creation of a standard 'Earth' topography for use in many future annuli studies.

[3] This paper appears to change the meaning of 'meta-stable' from '*can* transition from one regime to another', to '*will* transition between the regimes'. Hence, the 'meta-stable' states in Charney and DeVore (1979), that allow multiple equilibria, are re-classified as 'stable' by Tian et al (2001).

In a similar vein to the search for 'realistic' topography, an unresolved question exists in what type of topography should be employed. Practically all differentially heated annuli use sinusoidal topography. However, this can range from a simple wavenumber-2 type, as seen in Bernardet et al (1990), through a simple wavenumber-3 type shown in Risch (1999), to a non-axisymmetric wavenumber-5 type, found in Jonas (1981). A further option is for radial variation: Li, Kung and Pfeffer (1986) carried out experiments with radially uniform topography, but Leach (1981) included a slope so that his topography was greater near to the outer wall.

In numerical studies as well, a sinusoidal bottom surface as shown in Charney and DeVore (1979) is the most common. Again there is no standard, and both wavenumber-2, as in Li, Kung and Pfeffer (1986), and wavenumber-3, as in Molteni (1996), types are widespread, due to similarities to the topographies of Earth and Mars. Less regular shapes are also possible, such as Yang, Reinhold and Källén's (1997) single isolated mountain and Charney, Shukla and Mo's (1981) uneven topographic distribution based on actual measurements of Earth's mountain ranges.

Which choices are made are up to each individual author's judgement of what arrangement of equipment creates a good simulation of the atmospheric circulation without over-simplification or over-complication. However, it stands to reason that some types of topography will produce better simulations of the Earth (or whichever planet is the focus of interest) than others. This leads back to the concept of the search for a standard 'Earth' topography – experiments could determine whether radially uniform or radially sloped topography (for example) was a better compromise between realism and manufacturing difficulty, and thus declare that to be the superior representation.

A number of unresolved questions about the effects of topography on the atmosphere could be posed on the more unusual findings of Risch (1999). A strange occurrence was found whereby, for low Taylor number and medium Rossby number (both defined in Chapter 3) flows, a wave-3 stationary wave was found to grow a fourth 'wave-lobe' (Figure 2.2) at low levels, but not at high levels. This could possibly be showing an example of blocking, and could be examined via further study of that region of parameter space. A second question concerns the understanding of stratospheric sudden warmings, a mysterious phenomena of the atmosphere, although they are known to be caused by seasonal variations. Changing the temperature difference over longer time-scales could mimic these seasonal variations, thus leading to a study of stratospheric sudden warmings. Finally, a lesser question is the relative scales of the effects of thermal and topographic forcing on the rise of stationary waves. This could be investigated by using insulating material (or similar) to only allow a temperature difference on the upper half of the annulus, hence comparing the thermally-forced upper half to the topographically-forced lower half.

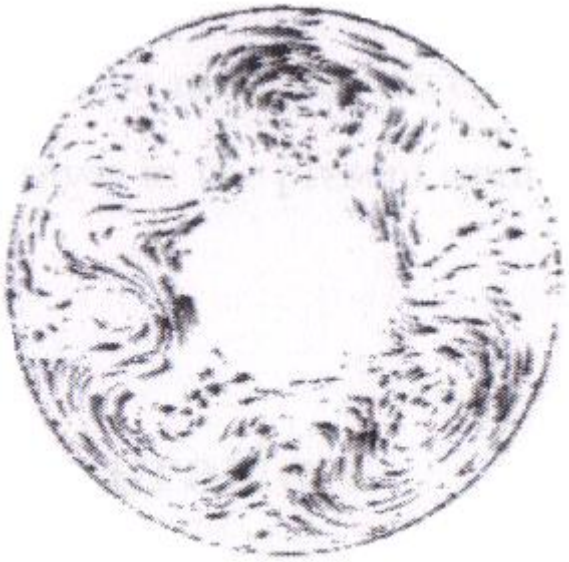

Figure 2.2: Wavenumber-3 structure with rogue 'wave-lobe' at low level, $\mathcal{T} = 1.2x10^6$ *[from Risch (1999)]*

Unfortunately, without a re-design of the annulus, the addition of insulating material for the forcing comparison experiment would cause interference with the flow, unless the material was very thin, at which point the insulating properties may not be strong enough to separate the thermal forcing. A fair amount of work would be needed to rectify this. The investigation into seasonal variations seems more feasible, with it also appearing to be a more interesting area of research and the most relevant to the atmosphere. Additionally, improving a laboratory study so that it more closely resembles the long-term atmospheric circulation would allow for study of oscillations with much longer periods than currently possible in a physical annulus. The rogue 'wave-lobe' discovered bears some similarity to the findings of the bifurcation study carried out in the first year of this project, so spatial period-doubling may be a cause. Future experiments with the same apparatus should be able to investigate this possibility further.

A more mathematical unresolved question, based on the comments of Benzi et al (1986), is that there is difficulty in writing full equations for the zonal flow over topography. This is due to a poor assumption for the calculation of form drag, a complicated feedback between topography waves and zonal wind, and the fact that non-geostrophic effects (such as boundary layer separation and topography steepness) are ignored.

Whilst form drag is a very interesting aspect of topography, with numerous parallels to other topics in fluid dynamics including nautical and aerospace engineering, a laboratory study such as an annulus cannot give an equation for zonal wind directly, like a numerical model could. However, a physical study could shed some light on which non-geostrophic parameters affect zonal wind, and by

how much. In addition, if time permits, the planned numerical study for the subsequent years of this thesis (see Chapter 6) may be adapted to attempt to answer this question.

A recent open question concerns the origin of Low-Frequency Variability (alternatively Low-Frequency Vacillation, shortened to LFV). LFV is defined by Koo and Ghil (2002) as the variability of the atmosphere with a time scale longer than major weather phenomena (5-6 days) but shorter than seasonal variability (about 100 days). Naturally, this means that the variability is extremely important for weather predictions and forecasting. The authors state that it is dominated by atmospheric zonal flow vacillation, and that it is often caused by non-linear interactions and transitions between multiple equilibria regimes, but the precise mechanism for its formation is still unresolved.

In a related subject to the above, Ghil and Robertson (2002) divided the topic of LFV into planetary flow regimes ("particles") and intraseasonal oscillations ("waves"). They state that it is unknown whether the former are slow phases of the latter, or the latter are instabilities of the former. The authors note that both are fundamentally important, and knowing their relationship will greatly increase predictability of the atmosphere.

Kondrashov, Ide and Ghil (2004) revisited this latter issue, seemingly leaning towards the idea that the slow phases of the oscillations denote the locations of the unstable equilibria, but decide that an in-depth analysis is "beyond the purpose of the present paper".

The origins and internal relationships of LFV would be a difficult question to answer in an annulus, though the topographically forced oscillatory instability discussed by Ghil and associates could be looked at in further detail. The transitions between regimes in the annulus and their counterparts in the atmosphere could also be studied, perhaps as part of a larger study into multiple equilibria.

Despite plentiful research in the area, a question remains of the precise effects of adding a small amount of topographic variation, as opposed to a flow over a flat surface. One of the most surprising and unusual effects of topography known from numerical models, for example Charney and DeVore (1979), is that low topography can actually act to stabilise a given flow, requiring a greater thermal forcing (or rotation rate, depending on what parameter is held constant) to produce instabilities. Cehelsky and Tung (1987) provide Figure 2.3 to illustrate this concept.

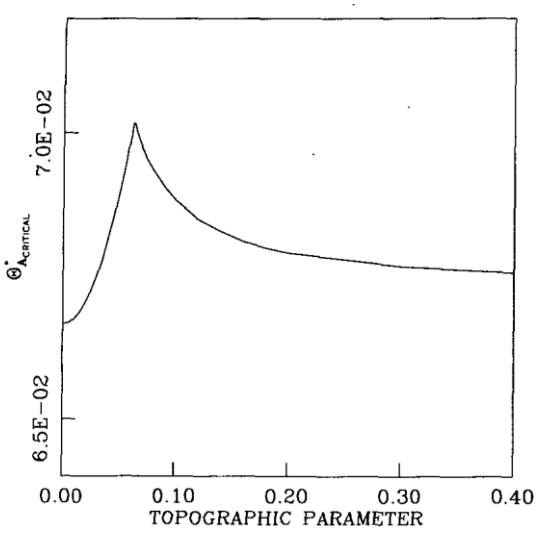

Figure 2.3: Representation of flow stability (represented by the y-axis, a higher value implying greater stability) against a dimensionless topographic height scaled by depth of fluid (x-axis) showing initial stabilisation and peak at low topography [from Cehelsky and Tung (1987)]

Jonas (1981) was the first to attempt to apply this effect to a physical annulus, using an increase in rotation rate rather than an increase in thermal forcing. Using a simple analysis, the author predicted the effects of the addition of topography, including an increase in rotation needed before the transition to baroclinic waves is reached, an increase in wavenumber of these waves and a decrease in length of the baroclinic waves. The predictions were backed up by the observations taken, but only qualitatively. The author noted that the analysis is "grossly inaccurate" when applied to the real annulus, not least because upper and lower boundary-layer separation (which would imply zero vertical velocity at the top and bottom) cannot be observed. He also mentioned that: "calculations of the spatial growth rates of perturbations in flows of spatially varying static stability would provide useful information on this mechanism".

Both blocking and zonal flow regimes with low topography were investigated in Tian et al (2000), with focus on their spatial and temporal characteristics. A numerical study is compared with a laboratory annulus, noting the spatial similarity of both experiments, including the shape and location of the flow vortices and the configuration and magnitude of the jet. No growth rate is given, however, and the annulus is barotropic – forced by rings of holes between the topography that pump in fluid to create an eastward jet.

As such, there is plenty of scope to investigate Jonas' (1981) findings with a differentially heated baroclinic annulus, focussing on the study of the spatial growth rates of the perturbations evoked. As noted by Jonas, it is very difficult to explore the separation at the boundary layers, but could be achieved (in a re-designed annulus) by having a lighting layer very close to the top or bottom of the fluid, and perhaps utilising an angled camera, such as in the boundary layer study. This solution

would have further problems, such as reflections from the lid, but would make for an interesting, if complicated, investigation.

As mentioned, Tian et al (2001) carried out their research with a different type of annulus – the barotropic annulus, shown in Figure 2.4. Instead of setting up convection via a temperature difference, a barotropic annulus creates a flow by pumping fluid through several concentric rings of holes that lie between the topographic peaks and troughs. This has the effect of removing any vertical variation and is employed when the stratification of the atmosphere is deemed negligible. Naturally, this removes complexity from the model, allowing other phenomena to be more easily observed.

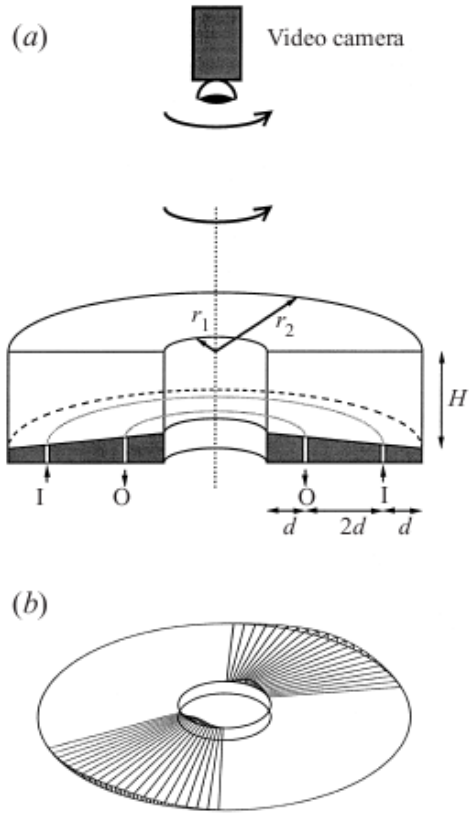

Figure 2.4: Barotropic annulus with sloping base a.) shows typical laboratory arrangement, b.) shows concentric rings of hole for pumping of fluid [from Tian et al (2001)]

The numerical equivalent to the barotropic annulus is the one-layer model, compared to the two-layer baroclinic model. One-layer models reduce the simulation to barotropic to decrease computational expense when vertical structure is not needed. This type of model is almost as common as the two-layer type, with examples occurring in Charney and DeVore (1979) and Benzi et al (1986). One-layer models also appear to be the standard for studies of Martian topography, with both

Keppenne (1992) and Keppenne and Ingersoll (1995) using barotropic shallow-water experiments in their papers.

This raises the obvious question – how far do barotropic and baroclinic models with topography differ? Furthermore, how does adding baroclinic structure affect the results of barotropic models? This could be investigated by replicating the results of Tian et al (2001) in a baroclinic annulus, or by using a one-layer numerical model under the same parameters as an annulus experiment.

Finally, it should be noted that, since the focus of this project is the interactions of topography with the atmospheric circulation, the majority of the literature examined is based on the dynamics of the atmosphere. The oceans experience topography as well and there is plenty of scope for comparison between the two. One of the major differences is the forcing of the flow: atmospheric studies, like all those mentioned above, are thermally-driven; oceanic studies, like Völker (1999) who simulated the Antarctic Circumpolar Circulation, are wind-driven. Without that distinction, the latter's study is difficult to distinguish from a standard atmospheric study, employing a baroclinic quasi-geostrophic channel model.

This being the case, it would form an interesting study to compare the oceans and the atmosphere within the annulus. This could be achieved by creating simple ocean-like topography, for example tall 'blocks' that could be dropped into the annulus, trapping the bottom layer, like the ocean basin experiments of Wordsworth (2008), except in that case the vertical walls used blocked the entire depth of the fluid. Alternatively, the ocean forcing could be simulated by replacing the heating and cooling systems with an array of fans to drive the flow. The current annulus in use would probably not make the best choice for either of these options (especially not the latter) due to its large size, but a smaller annulus could be converted relatively quickly and easily.

2.2 Proposed Topographic Studies

In conclusion, the existence of multiple equilibria is still the biggest unresolved question in topography, even if it is not as controversial a topic as it once was in the period after Tung and Rosenthal (1985) and Cehelsky and Tung (1987) published their papers. However, the most immediate aspect of this issue is how best to create a topography for an annulus that can be defined as 'realistic'[4]. This issue was brought up in Li, Kung and Pfeffer (1986). In that paper, a simple wavenumber-2 type topography was employed, but it is noted that the real topographic distribution of Earth (and other planets) is much more complicated. The authors expressed a wish to repeat their experiments with a better model of this distribution, suggesting a superposition of the Fourier components of wavenumber-1 and wavenumber-2. Taking the idea of an improved topographic distribution was brought to its logical conclusion in Boyer and Chen (1987), where one mountain range in particular, in this case the Rocky Mountains, was modelled in great detail for a laboratory experiment. Conversely, however, this paper was criticised for bringing *too much* complexity to such a simple simulation of the atmosphere. James (1988), for example, noted that having such a detailed topography was of dubious worth when the walls of the annulus will produce reflection patterns that simply do not exist in the flow over the Rocky Mountains. From this, the lesson learnt is that less-idealised topography should not be a hyper-realistic reproduction of a planet's surface. Instead, a smaller change to basic sine wave topography is needed, to reflect the limitations of the physical annulus model. As such, the original idea of Li, Kung and Pfeffer (1986) can be revisited: using a superposition of wavenumbers to create a less-idealised distribution.

Hence, part of the experimental investigation of this thesis will be a study into the various superpositions of the first three wavenumbers, especially in comparison to a simple sinusoid. In addition, the results of experiments under less-idealised topography may also go some way to answering the open questions of the previous section, such as the growth-rate and time-scale of the various topographically forced oscillations and perturbations, the existence of multiple equilibria with less idealised topography and the mechanism of generation of LFV.

From the literature, the second biggest unresolved question regarding topography appears to be that of blocking. Blocking's importance to the atmospheric circulation has been noted as early as Berggren, Bolin and Rossby (1949), who describe the synoptic-scale disturbances that affect both the local weather and the climate. Despite this, the blocking state is not very well understood, which is why it sometimes used as explanations of other phenomena, such as Risch's (1999) rogue wave-lobe.

[4] For the sake of clarity, instead of the term 'realistic', from now on the topography investigated will be referred to as 'less-idealised'.

It is known, however, that topography and blocking are inherently linked; for example Luo (2005) states that large-scale topography acts to lock a blocking flow to a single geographical position, hence creating a stationary wave. There are many ways to study blocking, especially when using numerical models, but within the annulus the best method of investigation, in terms of both simplicity and versatility, is via partial barrier experiments. Partial barriers serve to block part of the flow (either radially or vertically), and, in contrast to Wordsworth's (2008) previously mentioned ocean basin experiments (shown in Figure 2.5), allow comparison between blocked and unblocked flow. Partial barrier experiments should be quick and easy to set up, required only a minimum amount of topography, and offer straight-forward combination with other experiments. The physical structure of a partial barrier most resembles that of a continental shelf on the ocean basin - this will permit a focus on oceanic topography. The flow around continental shelves is of great interest in the literature, with many works studying the upwelling or downwelling (Federiuk and Allen (1995) and Allen and Newberger (1996), respectively) and the internal wave characteristics (Huthnancea (1989), for example) of the circulation influenced by this type of topography. Furthermore, as Allen (1980) points out: "sediment transport and pollutant dispersion are other processes occurring over the shelf that are strongly affected by the properties of the fluid motion."

As such, another set of this thesis' experiments will explore partial barriers in the annulus and will be employed to study both blocking and the effects of continental shelves on the ocean basin. In addition, a better characterisation of the blocking regime will also help with unresolved questions about multiple equilibrium, as described previously.

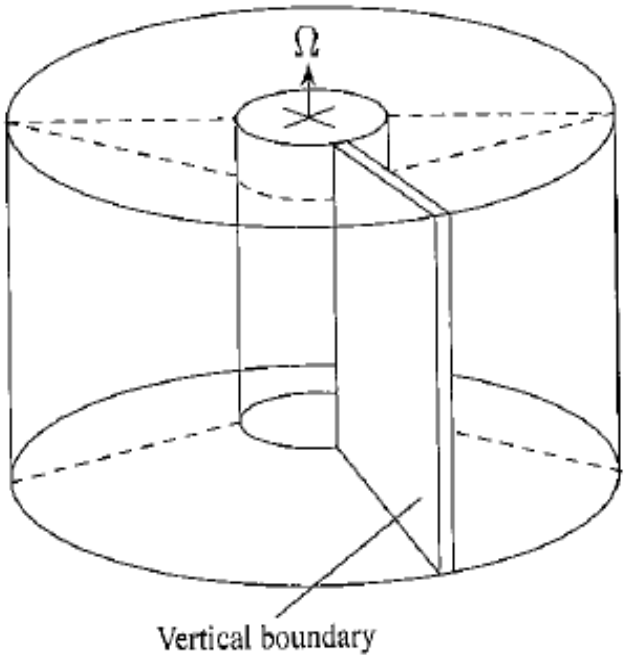

Figure 2.5: Ocean basin experimental arrangement, from Wordsworth (2008)

A rarer type of topography in the literature is that of 'thermal topography' – this is the technique of using differential heating in the azimuthal direction of the annulus. As mentioned by Risch (1999), it can be thought of as a parallel to mechanical topography, and there is a direct comparison to be found between the two. This should provide interesting results, merely by conducting thermal topography experiments in the same parameter space as those discussed above. In this way, it can be determined which type of forcing has a greater impact on the general circulation[5]. In the annulus, thermal topography can be employed to recreate the differential heating caused by the thermal differences between land and sea. This effect is felt most strongly in the tropics, where the flow generated is known as the Walker Circulation. Due to its comparative weakness throughout most of the year, the Walker Circulation is not as well understood as more major atmospheric processes like the Hadley Cell, but Boubnov, Golitsyn and Senatorsky (1991) note that, during the winter, "the temperature contrast between continents and oceans is of the same order as the temperature difference between tropical and polar regions." It is hoped that thermal topography may improve knowledge of this process. The azimuthally-varying heating can be used to simulate other planets as well, such as Mars, as in Nayvelt, Gierasch and Cook (1997), where the surface can act as heat sources and sinks due to short radiative timescales. Adaptations to the study of tidally-locked exoplanets are also possible, but are outside the scope of this study, due to the numerous alterations that would have to be made to the annulus.

Thus, the remainder of the experiments of this thesis will investigate thermal topography, especially with regard to examining an analogue of the Walker Circulation and comparing results with the mechanical topography studies. The latter should allow context for those results, in turn permitting superior characterisation of topographically forced oscillations and perturbations.

[5] For a brief discussion of thermal versus topographic forcing on Eastern continental boundaries, see Kaspi & Schneider (2011).

Chapter 3

Experimental Arrangement

This chapter will first explain the apparatus available for this project's investigation, split up into the experimental equipment itself and all the hardware and software needed to actually generate results. The next section will detail the process of how everything was put together, and the final section will describe how the equipment will be employed to achieve meaningful solutions to the problems posed in the previous chapter. Details of the topography specially designed for this project will also be discussed. First of all, however, a brief introduction to some of the more relevant dimensionless numbers will be provided, in order to give context to the parameter space under investigation.

3.1 Non-dimensional Numbers

Whilst the flow of the atmospheric circulation is extremely complicated, for typical annuli experiments (and computational annulus models) the entire system can be reduced to two dimensionless numbers which fully describe parameter space. Firstly, the Taylor Number is defined as:

$$\mathcal{T} = \left(\frac{f \cdot L^2}{\nu}\right)^2 \tag{3.1}$$

where L is the characteristic length scale and ν is the kinematic viscosity. The Coriolis Parameter, f, also known as the Coriolis Frequency, describes the effect of the planetary rotation (ω) depending on latitude (φ) and is found using the equation:

$$f = 2\omega \cdot \sin(\varphi) \tag{3.2}$$

For an annulus experiment, φ is taken to be 90°, and the Taylor Number can be adapted[6] to the form:

$$\mathcal{T} = \frac{4\Omega^2 (b-a)^5}{\nu^2 \cdot d} \tag{3.3}$$

[6] As described in Fowlis and Hide (1965).

where a is the inner radius, b is the outer radius and d is the height of the annulus and Ω is the rate of rotation of the fluid. Roughly, the Taylor Number gives the ratio of the Coriolis forces (the numerator) to the viscous forces (the denominator) acting upon a fluid. A large value implies a less stable flow, with circulation tending toward higher dominant wavenumbers and the irregular regime.

Secondly, the Rossby Number is defined as:

$$\theta = \frac{U}{f \cdot L} \tag{3.4}$$

where U is the characteristic velocity scale of the fluid. For an annulus experiment, this can be adapted[7] into the Thermal Rossby Number (sometimes also known as the Hide Number, hereafter simply 'the Rossby Number') which takes the form:

$$\theta = \frac{\alpha \cdot g \cdot d \cdot \Delta T}{\Omega^2 (b-a)^2} \tag{3.5}$$

where α is the thermal expansion coefficient, g is the gravitational acceleration and ΔT is the temperature difference. Roughly, the Rossby Number gives the ratio of the inertial forces (the numerator) to the Coriolis forces (the denominator) acting upon a fluid. At large values the quasi-geostrophic approximation begins to break down, leading to Houghton (2002) to refer to the Rossby Number as a "measure of the validity of the geostrophic approximation".

As most of the quantities are assumed (or fixed) to be constant, the Taylor Number can be simplified to being proportional to Ω^2, and the Rossby Number can be simplified to being proportional to $\frac{\Delta T}{\Omega^2}$. For an annulus experiment (or similar) the rotation rate and the temperature difference are the main sources of control, hence, these two dimensionless numbers can be taken to fully describe the parameter space that the experiments take place within, as noted by Hide and Mason (1975) in their pioneering study of the annulus.

3.2 Equipment Description

Accounts of the experimental arrangement in question can be found in the theses of two of its previous users - Risch (1999) and Wordsworth (2008). The latter is more helpful, as it is more recent (thus the electronics are more up-to-date) and Wordsworth made several changes to the annulus, replacing the O-ring seals and decreasing the radius of the inner cylinder to permit higher Taylor Numbers to be reached. Figure 3.1 provides two labelled photographs of the annulus, illustrating the apparatus described in this chapter.

[7] A full derivation can be found in Holton (1992), for example.

a.)

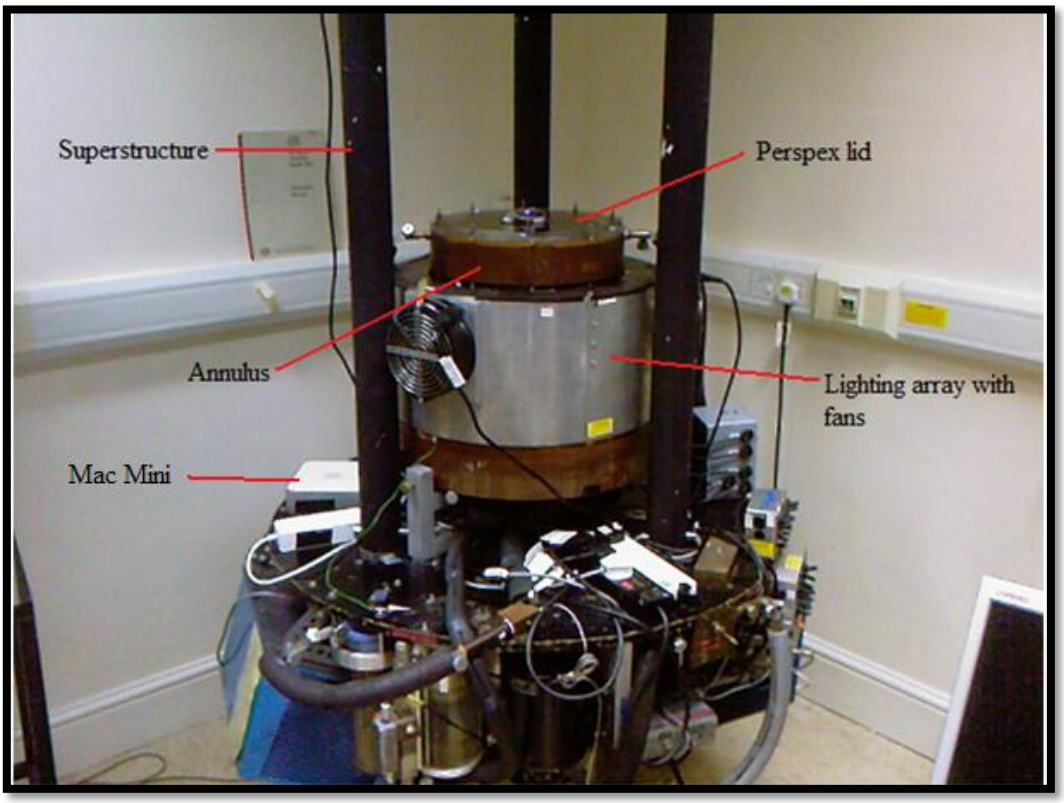

b.)

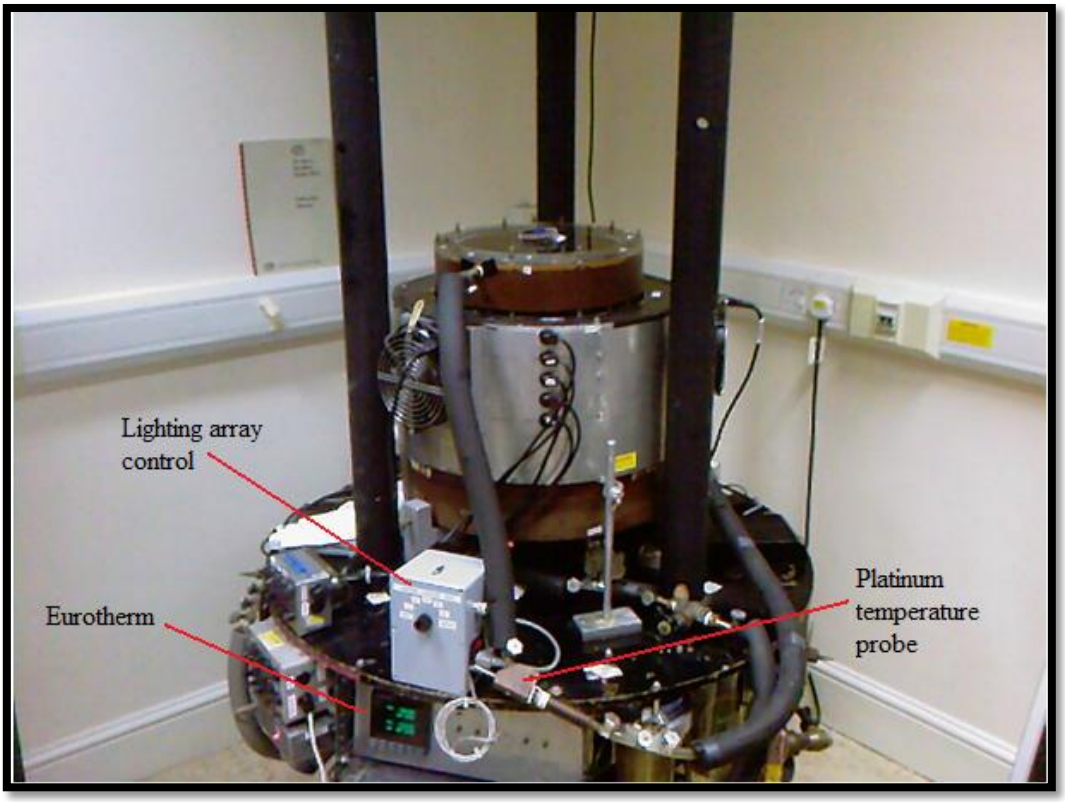

Figure 3.1: Annotated photographs of the annulus from two different sides, with apparatus arranged for the bifurcation study.

As explained in Chapter 1, an annulus functions by setting up a temperature difference between the heated outer edge and the cooled inner cylinder. This is achieved via two flows of water that each travel through a separate circuit containing a pump, a refrigerator, a heater, a filter and a platinum temperature probe. A feedback system between the probes and a Eurotherm 900 EPC Temperature Controller manipulates the temperature of the water entering the outer edge or the inner cylinder to any specified value. The entire organisation is shown in Figure 3.2.

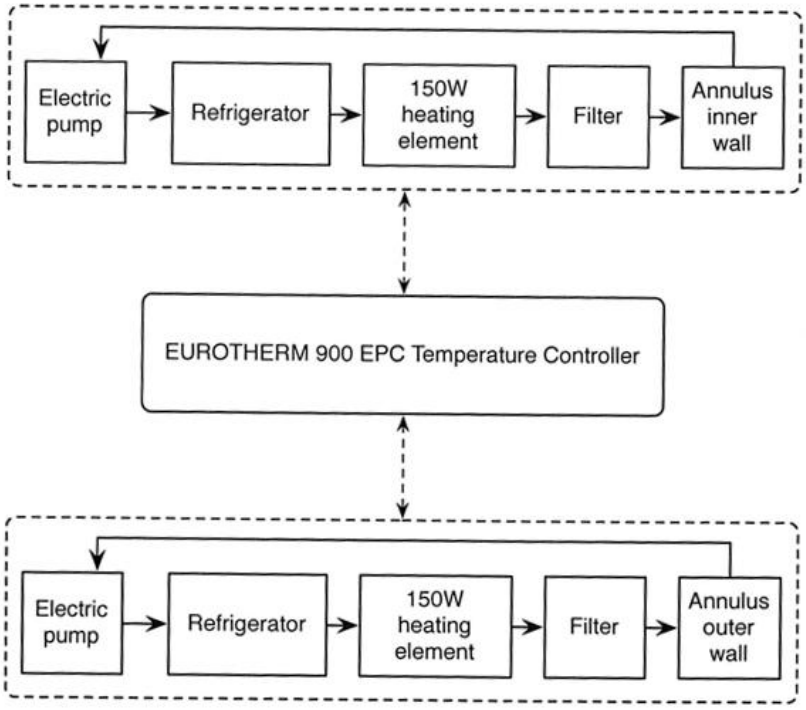

Figure 3.2: Block diagram of heating and cooling flow circuits and feedback system [from Wordsworth (2008)]

The annulus itself is made of Bear grade Tufnol, a resin-bonded multi-layer fabric, and brass, both materials chosen for their thermal properties. The rigid lid is kept in contact with the working fluid and is made of Perspex, for its transparency. The working fluid is a mixture of water and glycerol, made up so that its density is 1.044 kg m^{-3} (the exact ratio of compounds was deemed unimportant, but will be roughly 17% glycerol). This density allows 350-500 μm pliolite tracer particles to be neutrally buoyant. It was decided that the value of $1.66x10^{-6}$ m^2s^{-1} for kinematic viscosity used by other studies employing this mixture[8] was inaccurate. Hence, a sample of working fluid was examined in a viscometer, giving a new result of $1.58x10^{-6}$ m^2s^{-1}. A solution known as Sanosil S006 was added to the fluid to prevent mould growth. The lid and the inside of the annulus were also treated with this solution. An array of thirty 50 W halogen lamps over five layers surrounds the annulus, allowing light to pass through transparent slits at those layers. This is illustrated by Figure 3.3.

[8] Taken initially from Hignett et al (1985).

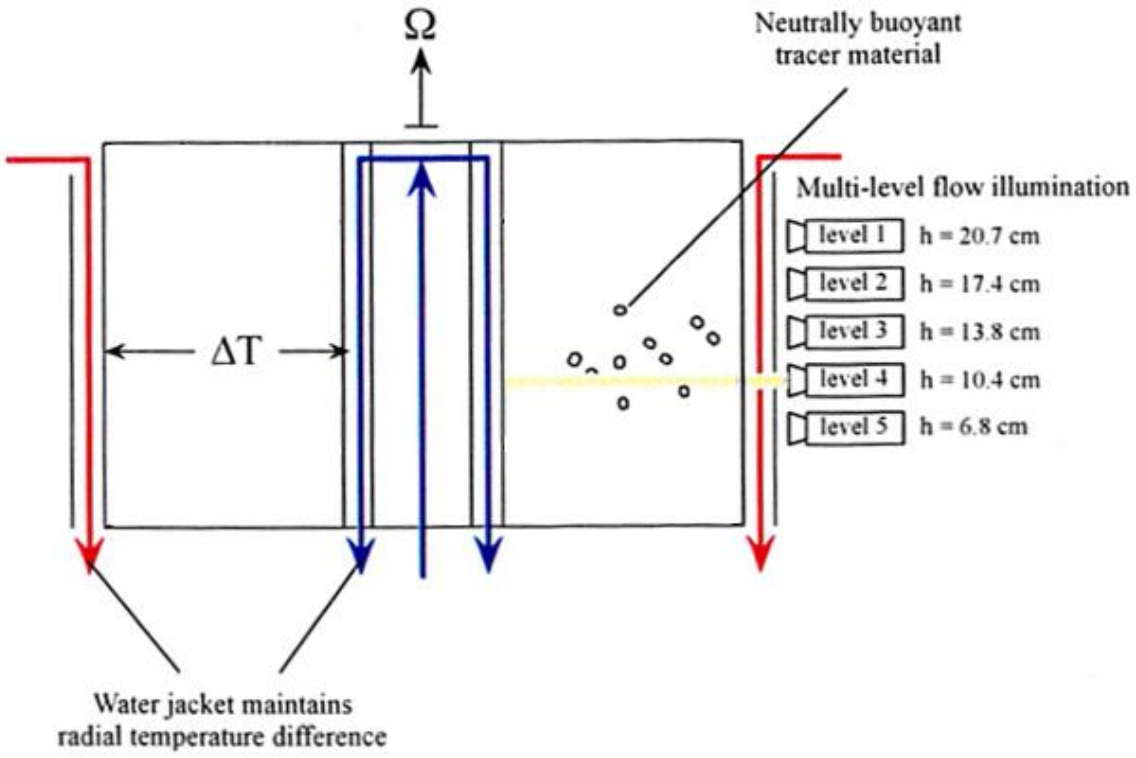

Figure 3.3: Schematic of the lighting array and heating system in side view [adapted from Wordsworth (2008)]

Due to the nature of the halogen lamps, which are very prone to overheating and thus also causing an additional heat source on the outer edge, three large electric fans were attached to the lighting array. An electronic control box controls which of the five layers is illuminated at a time, with an option for an automatic shift between them at a variable rate. A camera is mounted above the annulus on a tripod-shaped superstructure, with a cone blocking all outside light between it and the Perspex lid. With this arrangement, the camera can see the motion of the tracer particles, and thus the flow structure, at any one of the five levels in Figure 3.3. By switching quickly between the layers, the vertical structure can also be resolved.

The annulus to be used is a larger model than the standard, as it was designed for use at high Taylor Numbers. Its dimensions, as well as several other relevant experimental parameters, are given in Table 3.1.

Table 3.1: Important experimental parameters

Radius of Inner Cylinder	a	4.5 cm
Radius of Outer Cylinder	b	14.3 cm
Depth of Annulus	d	26.5 cm
Kinematic Viscosity of Water	ν_w	$1.004x10^{-6}$ m^2s^{-1}
Thermal Expansion Coefficient of Water	α_w	$2.07x10^{-4}$ K^{-1}
Density of Water-Glycerol Mixture	ρ_g	1.044 kgm^{-3}
Kinematic Viscosity of Water-Glycerol Mixture	ν_g	$1.58x10^{-6}$ m^2s^{-1}
Thermal Expansion Coefficient of Water-Glycerol Mixture	α_g	$3.16x10^{-4}$ K^{-1}

3.2.1 Data Acquisition

In deference to previous set-ups, a Firewire (type: DFK 31BF03) camera was selected for taking visual results, due to its high picture quality and supposed simplicity of connection with a Mac Mini computer. The Mac Mini, a recent model, is small and light enough to be mounted to the rotating frame, and saved the images and movies to a 500 Gb Seagate Hard Drive. A Local Area Network (LAN) was set up to allow it to communicate with a second computer in the laboratory frame. This stationary computer, a Dell 780 MT 2.66 GHz Core Quad, is known as the 'base station'.

In terms of software, the free TightVNC (Virtual Network Client) package allows the base station to remotely control the Mac Mini, and therefore the camera functions. The digital signal from the camera is picked up on the base station by a software program called BTV Pro, which takes movies of the flow in motion and makes hundreds of frame-by-frame images from them. BTV Pro also ensures the gain of the camera is constant, so that each image occurs under the same conditions. These images are then transferred to a MATLAB program called Coriolis, an example of Correlation Image Velocimetry (CIV) – an iterative algorithm that tracks the translation, rotation and shear motion of the tracer particles. From this information, CIV creates a velocity vector field of the flow, with the option of manually removing any false readings. Modal analysis of the vector field should prove extremely important for detailed examination of the fluid structure, including the ability to create delay coordinate reconstructions.

In addition, a LabVIEW control system was created to give precise, continuous management over the rotation of the annulus. A similar thermal control system is under development to wirelessly direct the Eurotherm 900, but encountered problems due to the age of said equipment. Both control systems can be accessed from the base station.

3.3 Process of Re-building and Issues

When the project began, the apparatus had been taken apart to make space for other experiments. Hence, the major task of the first year of work was to restore the equipment to such a point where experiments could be carried out. Before any of this could begin, however, the turntable was tested for an inherent 'wobble' noted by Wordsworth (2008). A bowl of water was placed in the center of the turntable, to see if any asymmetric ripples could be observed. As none were found, it was decided that the reported vibration must have been due to a section of plumbing rubbing against the structure as it rotated. When the re-build was complete, a second vibration test was carried out, once again finding the 'wobble' to be negligible.

To ensure the annulus was positioned exactly in the center of the turntable, an optical cathetometer (also known as a tracking telescope) was employed. Warping of the wooden annulus base caused a small deviation to the rotation, measured by a Baty Dial Test Indicator to have a maximum of roughly 1.5 mm. As this deviation was confined to the base, not the outer or inner cylinders, this was judged to be negligible.

Once all the components were fixed in the correct location, the process of connecting up the plumbing could begin. All the previous pipes and insulation had been lost or discarded when the apparatus was taken apart, so the entire water system was replaced with new material. During this time various leaks were repaired as well as possible and the impellor for the outer cylinder pump was replaced. The electronics were next to be installed, with the camera, Mac Mini and hard drive attached to the superstructure and all those devices (and the fans, lights etc) were connected to the mains via a slip ring. Lastly, the Firewire camera needed a different attachment to the one used by Wordsworth (2008), so a new aluminium bracket was designed and built.

Unfortunately, midway through the control experiment (described in the next section), the Mac Mini suffered a fatal error and had to be retired. In its place, a Logitech Quickcam Pro 9000 Webcam was attached to an Optiplex 780 USFF computer on the rotating frame, to act as a temporary substitute until a more permanent replacement could be found. A MATLAB program was created employing the Image Acquisition Toolbox to create real-time streak-line images and movies from this camera. These results are excellent at characterising the type of flow at a given point: which wavenumber most resembles the motion, whether the waves are stationary or drifting and whether any kind of vacillation is observed. However, the streakline data cannot be modally analysed, and so permits less detailed examination of the flow. As such, when the permanent camera/computer replacement is installed, it is hoped that both vector velocity plots and streakline images can be achieved simultaneously.

3.4 Topographic Arrangement

This section will expand upon the basic experimental ideas put forward in the previous Chapter. The reasoning for the design of the topography that was built is given, as well as how this design influenced the arrangements for each experiment.

3.4.1 Wavenumber Superposition

For the superposition experiments it was noted that the Fourier decomposition of the Southern Hemisphere of Mars, from Hollingsworth and Barnes (1996), suggests that its topography appears to be formed from both a wavenumber-1 and a wavenumber-3. This is illustrated in Figure 3.4.

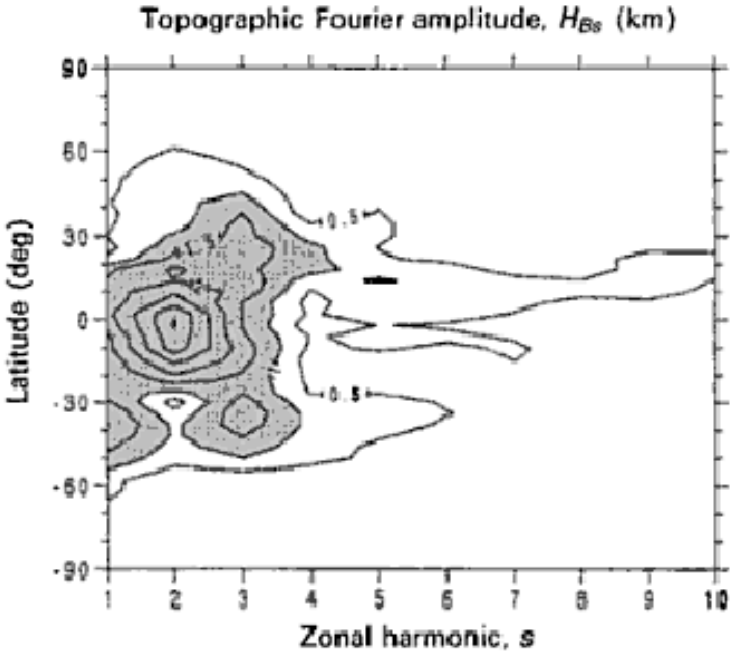

Figure 3.4: Fourier decomposition of Martian topography [from Read and Lewis (2004), created using a dataset by Hollingsworth and Barnes (1996)]

To verify this, a new Fourier analysis of the Martian topography was conducted (data taken from the LMD/UK Mars General Circulation Model LMD/UKMGCM), as shown in Figure 3.5. From this Figure it can be clearly observed that, at a certain latitude circle of about 40°S, wavenumber-1 and wavenumber-3 are dominant. Hence, ignoring lesser wavenumbers and utilising the amplitude and phase differences, a superposition of these wavenumbers was found, illustrated by Figure 3.6.

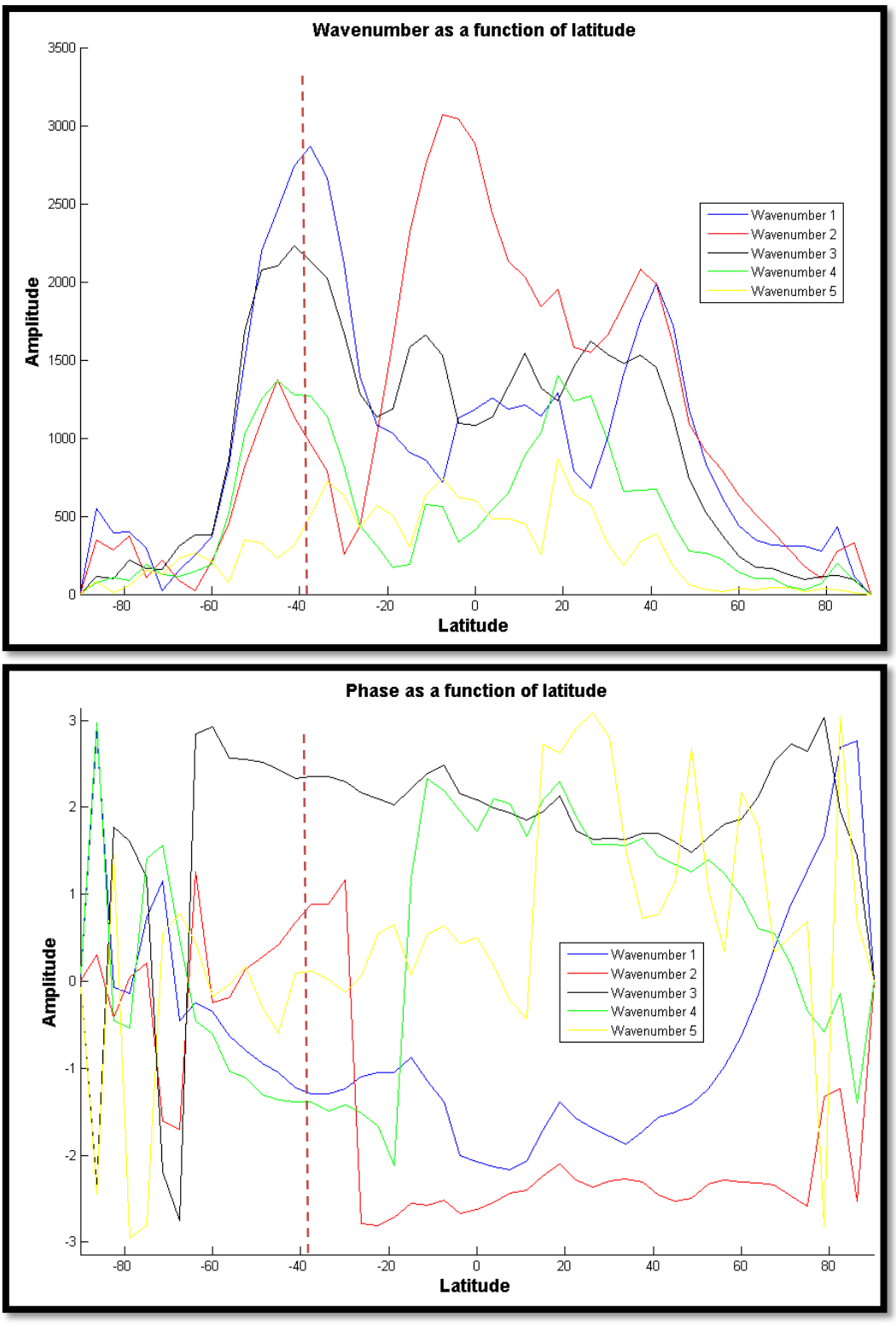

Figure 3.5: Fourier analysis of Martian topography, with red dotted line indicating latitude of interest

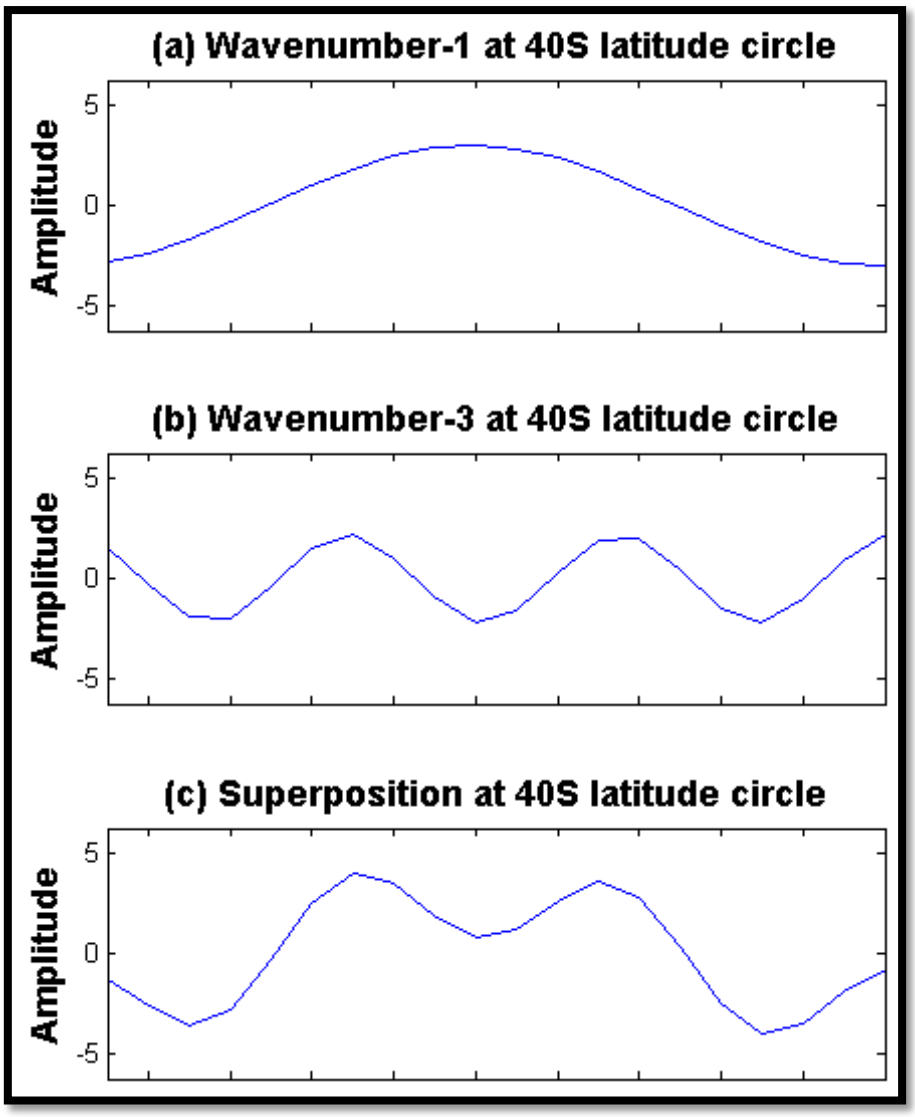

Figure 3.6: Illustration of superposition of two most dominant wavenumbers at the Martian 40°S latitude circle, determined from Fourier analysis of topography

However, it was decided that making an exact replica of the superposition in Figure 3.6 (c) would limit the flexibility of the experiments. Instead it was noticed that, due to its relative amplitude and phase position, the impact of the wavenumber-1 in (a) acts directly between two of the wavenumber-3 peaks in (b). In this way, the superposition somewhat resembles a wavenumber-3 topography in which two of the peaks are roughly twice the height of the other. Hence, three distinct Perspex bases were built (flat, low amplitude wavenumber-3 and high amplitude wavenumber-3), specifically designed so that they could be taken apart and re-assembled to form a variety of shapes. The three bases, as they were modelled in the CAD software Inventor, are shown in Figure 3.7. All three bases have an outer radius of 14.3 cm and an inner radius of 4.675 cm to allow a 2.5 mm gap from the sides of the annulus, in case of expansion of the Perspex. In addition, the minimum thickness of each base is 1 cm, to permit seamless inter-changeability.

a.)

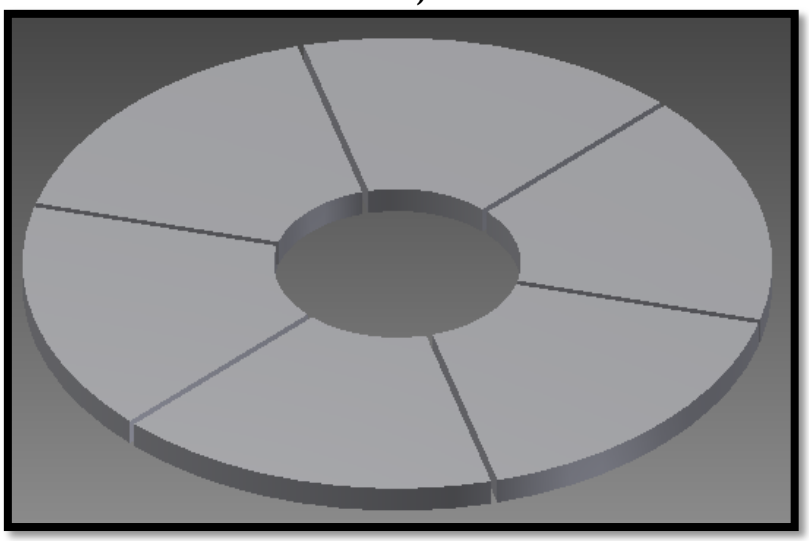

b.)

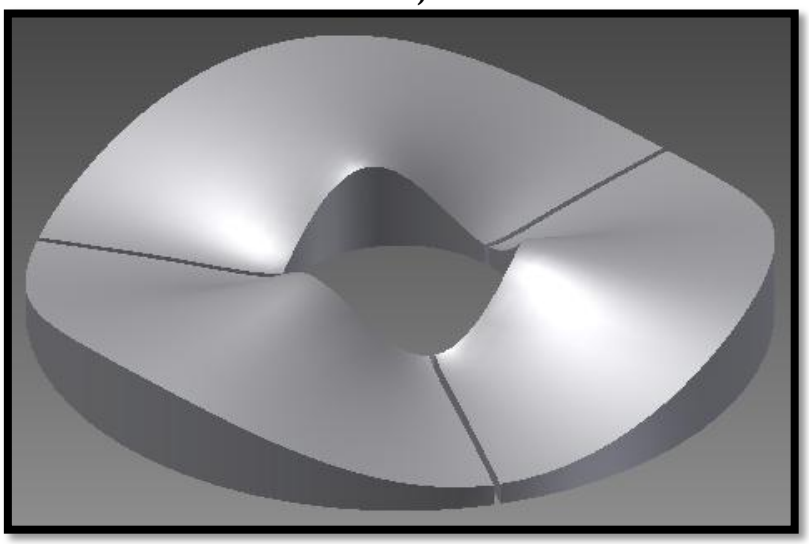

c.)

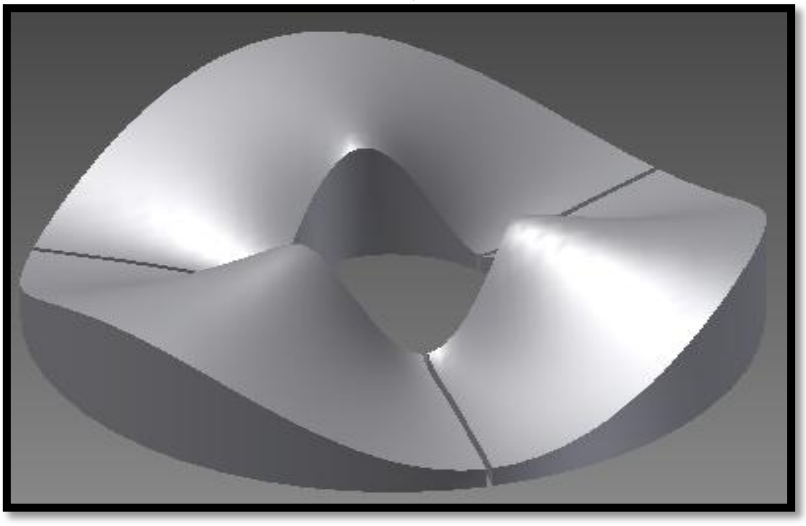

Figure 3.7: Topographic bases: (a) flat base, (b) low amplitude wavenumber-3 with maximum peak of 40 mm and (c) high amplitude wavenumber-3 with maximum peak of 60 mm.

To simulate the aforementioned Martian superposition in Figure 3.6 (c), the bases can be arranged as in Figure 3.8, where two of the high-amplitude peaks and one of the low-amplitude peaks combine to reflect impact of the wavenumber-1 in (a). It is hoped that this arrangement will not only allow the study of the effects of combining wavenumbers, but should furthermore give a rough model for the topography of the Southern Hemisphere of Mars.

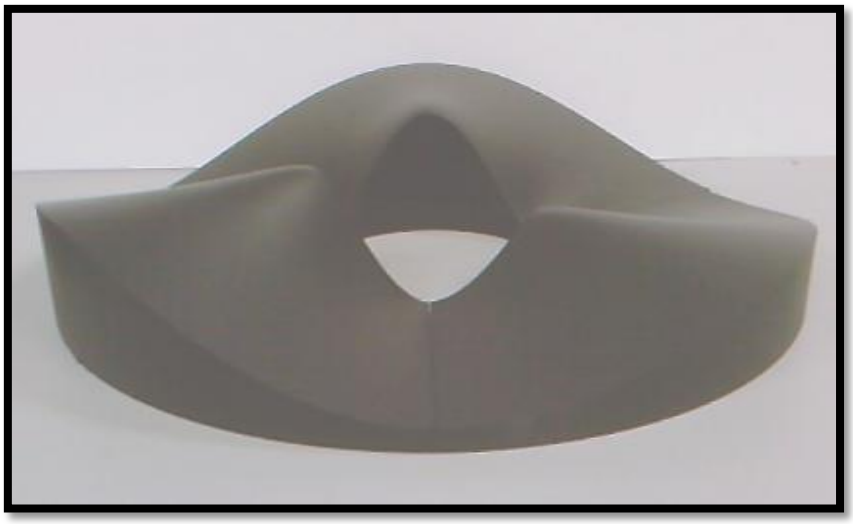

Figure 3.8: Bases arranged to produce superposition of wavenumber-1 and wavenumber-3

3.4.2 Partial Barriers

Since the topography to be built is in the form of wave-segments, it makes sense to use this opportunity to adapt the partial barrier experiment to that of an isolated ridge one. By combining the flat base with a single peak from one of the other bases, a vertical wall can be implemented, as illustrated in Figure 3.9. The height of the wall can be varied by simply swapping between whether the high or the low amplitude base is used for the single wave. This method removes the need for separate barriers to be made, and also allows for comparison of the effects of a curved wall with a sheer one (as utilised in previous works: Rayer, Johnson and Hide (1998) for example). As well as permitting the investigation of oceanic blocking, the curved wall is a more realistic simulation of blocking structures in the atmosphere, especially with regard to the topographic impact of the Andes in the Southern Hemisphere. If time allows, later experiments may also employ both sheer and curved walls simultaneously.

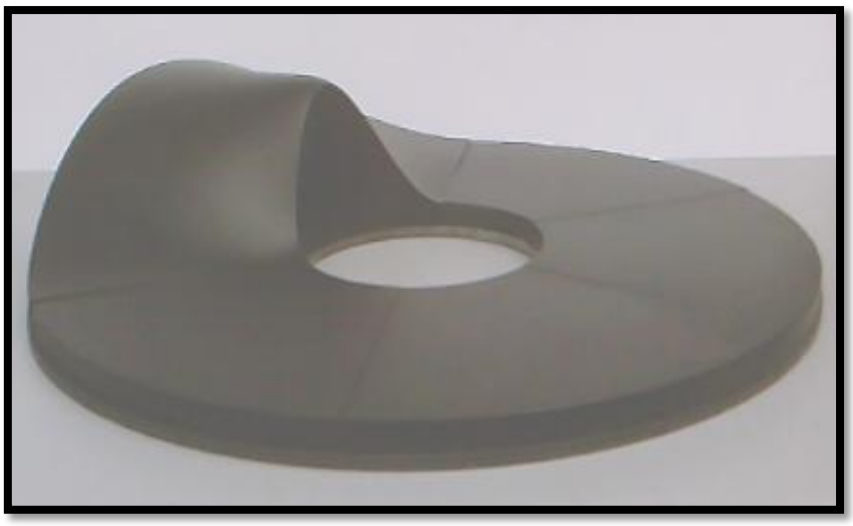

Figure 3.9: Bases arranged to produce a partial barrier

3.4.3 Thermal Topography

To achieve the azimuthally-varying heating profile needed for thermal topography, flat heating elements on the base of the annulus can be employed. These elements will be stretched from the inner to the outer wall over a sector one third of the area of the base, forming a rough parallel with a single peak of mechanical topography, as described in the partial barrier experiment. The elements in question are Kapton Insulated Flexible Heaters, chosen due to their flexibility, thinness (~ 1 mm) and water-proofing. The voltage across the elements can be altered, allowing a range of azimuthal thermal profiles for each radial thermal profile. Ten rectangular elements of 3 cm by 10 cm were purchased; each rated 10 W/in^2.

Thermal topography can also be combined with mechanical topography to create new experimental investigations. For example, using the elements with the isolated ridge arrangement would allow for study of monsoon events and Western Boundary Conditions. In addition, placing the elements on the ridges of the Martian superposition arrangement would give a parallel to the Martian topographic heating. Nayvelt, Gierasch and Cook (1997) note that, when no global dust storms are present, Mars has a simpler diabatic heating system than Earth, being mostly radiative in nature. On Earth, mountains are embedded in the background thermal structure, but on Mars the surface temperature is essentially uniform regardless of altitude. Hence, Martian mountains can act as heat sources and sinks, as well as obstructions to the flow. Heating elements on top of the topographic peaks should be able to simulate this effect.

3.4.4 Control Experiment

To create a reference point to which all the studies can be compared, it was decided that a control experiment with some simple sinusoidal topography would be employed. This control experiment would also be used to check the readings being obtained against a similar investigation in the literature. For this purpose, the recent studies of Read and Risch (2011) were chosen. Their topography was a wavenumber-3 style, with the peak at 3.1 cm and the trough at 0.9 cm. In turn, their annulus had an inner radius of 2.5 cm, outer radius of 8 cm and a mean depth of 12 cm. As this is roughly half the size of this investigation's annulus, using the high-amplitude wavenumber-3 topography (peak at 6 cm, with the trough at 1 cm) should match the topographic aspect ratio of those experiments. In order to compare results, the same parameter space location was examined, shown in Figure 3.10.

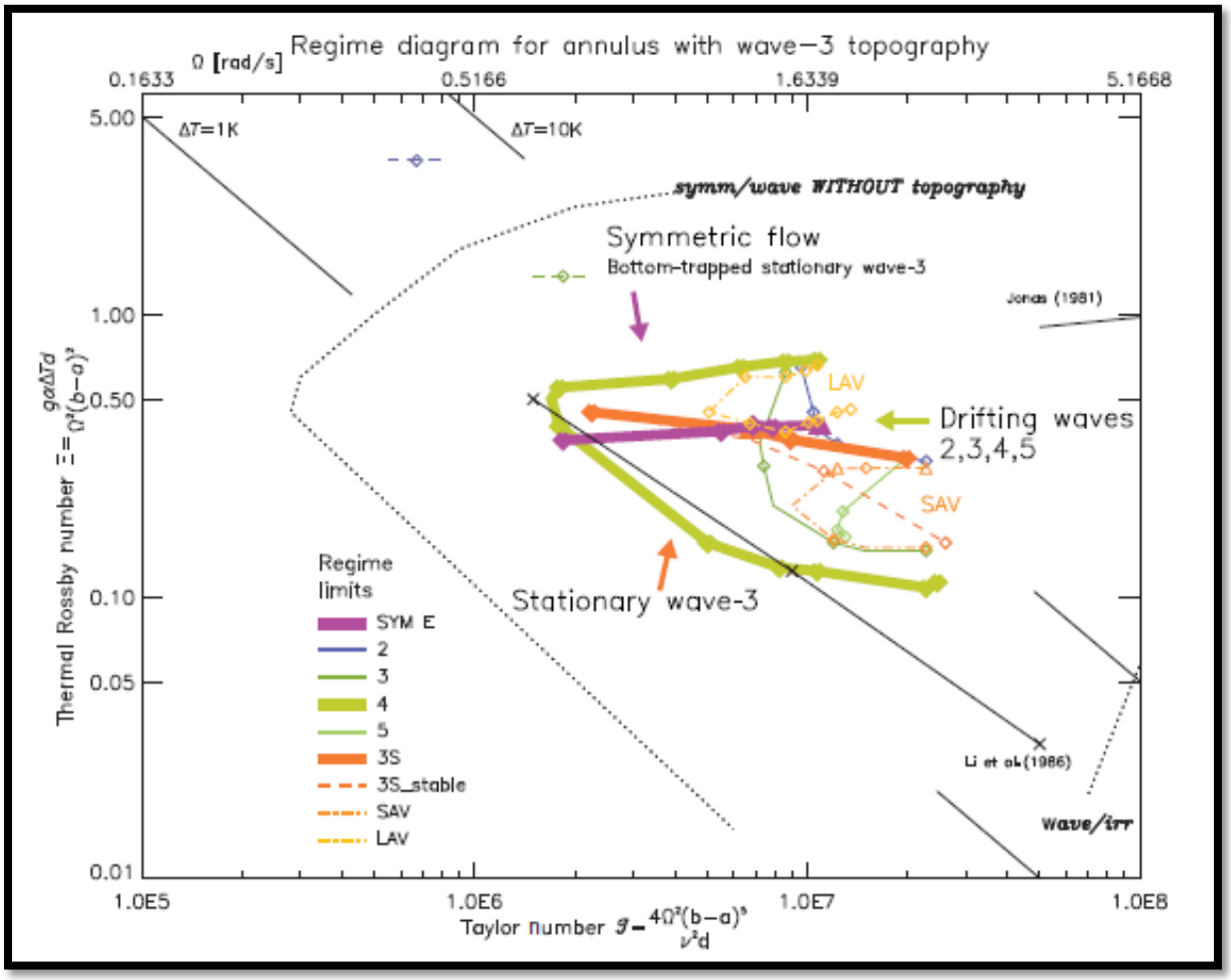

Figure 3.10: Regime diagram, showing parameter space to be investigated, from Read and Risch (2011)

It was initially hoped that the whole of the green-lined "anvil-shaped" structure could be explored. Unfortunately preliminary experiments found that, at these low rotation rates and temperature differences, the evolved wave structure was too weak to maintain the floating tracer, and most of the particles fell to the bottom of the annulus. This is because this project's annulus is significantly larger than that used by Read and Risch (2011), and was designed to be able to reach significantly greater Taylor Numbers. Instead, experiments were carried out as close as possible to the original studies, as shown in Figure 3.11, but with the extra option to explore additional parameter space at these higher Taylor Numbers.

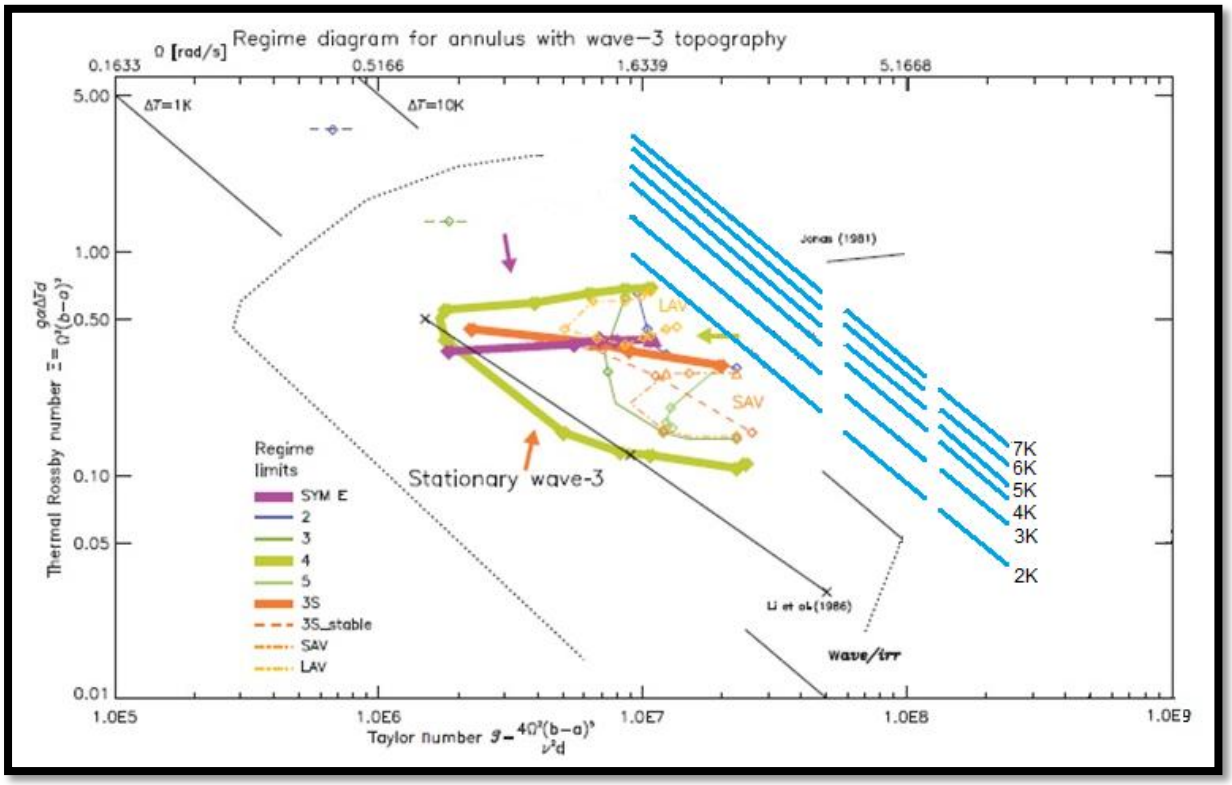

Figure 3.11: Extended regime diagram adapted from Read and Risch (2011), with highlighted area of investigation. Each blue line is a scan at a constant temperature difference.

Figure 3.11 shows three major regions: an axisymmetric regime above the top of the green 'anvil', a drifting wave regime within the 'anvil' and a stationary wavenumber-3 regime below it. There is also amplitude and structural vacillation evident at the upper and lower parts of the 'anvil', respectively. The control experiment will be used to check for all these flow structures, though it has been noted[9] that transitions may occur in different locations for different annuli. Once the control experiment is completed, this parameter space could then be used for all the other experiments

[9] By Hignett et al (1985), for example.

described above. By performing the same scans as shown in Figure 3.11 with the various different topographies, the corresponding effect on the observed flow regimes can be investigated.

2.5.5 Methodology

For each experiment, the relevant arrangement of topography is to be placed at the bottom of the annulus. The required density of water-glycerol mixture would then be added. To ensure particle saturation, the annulus would be sped up to an arbitrary high rotation rate before being slowed to the relevant speed under examination. The apparatus would be then left for one hour to allow the fluid to achieve solid-body rotation and to allow the wave structure to become fully baroclinic. After this point, results will be taken over the course of 60 minutes. In this way, an array of images will be taken via BTV Pro, allowing CIV to create velocity vector diagrams of the flow.

Due to the LabVIEW control system only working for the rotation rate, it was decided to perform scans of constant temperature difference and increasing rotation velocity to explore as much of parameter space as possible. Once a scan is finished, the annulus can be stopped, and a new scan at a larger temperature difference can be started.

For the control experiment, it was decided not to include baroclinic data by taking readings at different levels of the flow. As such, all images were taken at the clearest height – level 2, at 17.4 cm above the base (16.4 cm above the troughs of the topography). The other experiments will feature data taken from every level.

2.5.6 Planned Work Order

As previously mentioned, the physical topography was designed to be as flexible as possible, allowing an enormous range of possible experiments. For example, using the method of interchangeable bases, a much greater number of topographies can be examined, even including those without wavenumber-3 features, such as demonstrated in Figure 3.12.

Figure 3.12: Bases arranged to produce wave-2 topography

So great is the number of possible experiments, a definite plan of work was needed, ordering the studies by virtue of time needed to implement them against their expected payoffs in results. First of all, the control experiments will be carried out, both to compare with earlier experiments presented in Read and Risch (2011) and to set up a reference point for all the following studies. This will first be followed by the partial barriers experiments, judged to be the easiest to carry out to get some interesting early results. After these mechanical experiments have been carried out, purely thermal topography will be employed. After this, both topographic types will be used together in a variety of experiments. Next, the base will be replaced by the Martian superposition in Figure 3.8, as this experiment was decided to be the most time-intensive. Lastly, depending on the results found and the amount of time remaining, other combinations of bases and superpositions will be also investigated. This process of work is summarised in Figure 3.13.

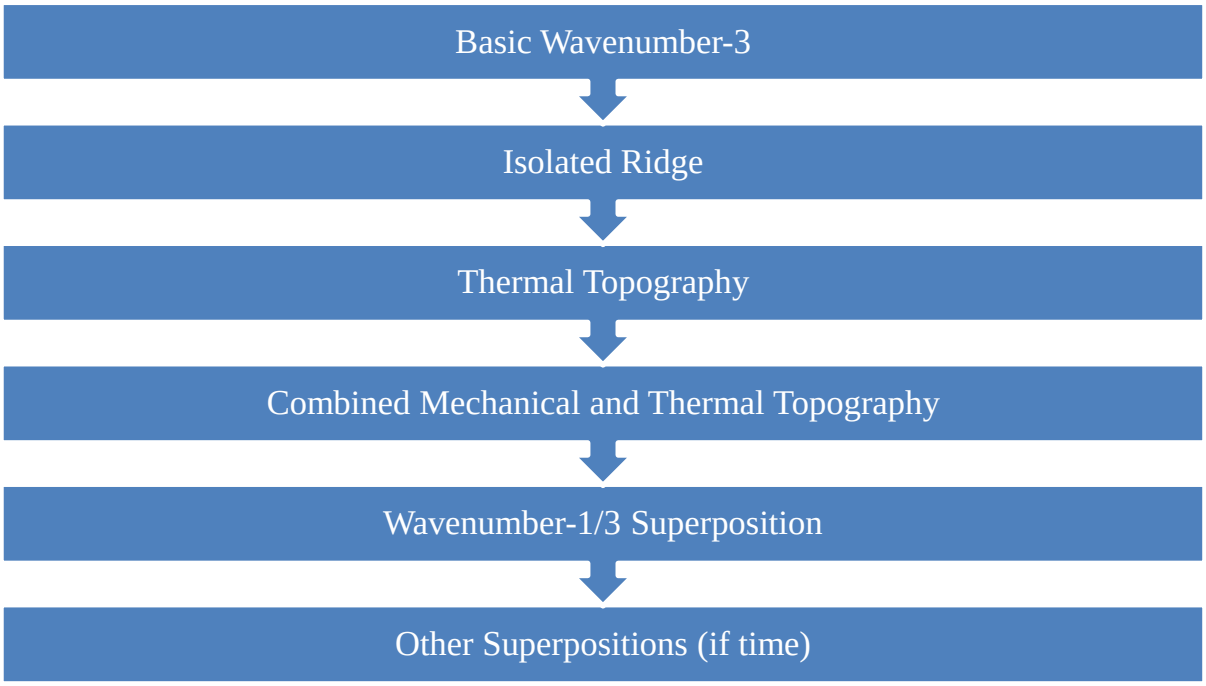

Figure 3.13: Planned order of investigation

Chapter 4

Results

The results of the various experiments completed thus far are contained within this chapter. At this stage, only the control experiment is fully finished, but preliminary readings from the partial barriers experiment have also been started. After each study, a short analysis will be given, describing what is observed and noting any trends discovered. More detail on the presented Figures will be explained in the introduction to each section.

4.1 Control Experiment

For each point in parameter space, three velocity vector images, each using CIV from two images separated by a time gap of one second, were created – the first just after the one hour spin up at 3600 s, the second 30 minutes after that at 5400 s, and the third another 30 minutes after that at 7200 s. Clearly anomalous or 'false' vectors flagged by the software were manually removed. Each Figure is marked with this time, as well as the rotation rate, temperature difference, Taylor Number and Rossby Number (dimensionless numbers calculated to 3s.f.). For sake of space and clarity, not every result that was taken will be given in this section. Instead, the regime diagram of Figure 4.11 will be updated with the dominant flow structure at each point.

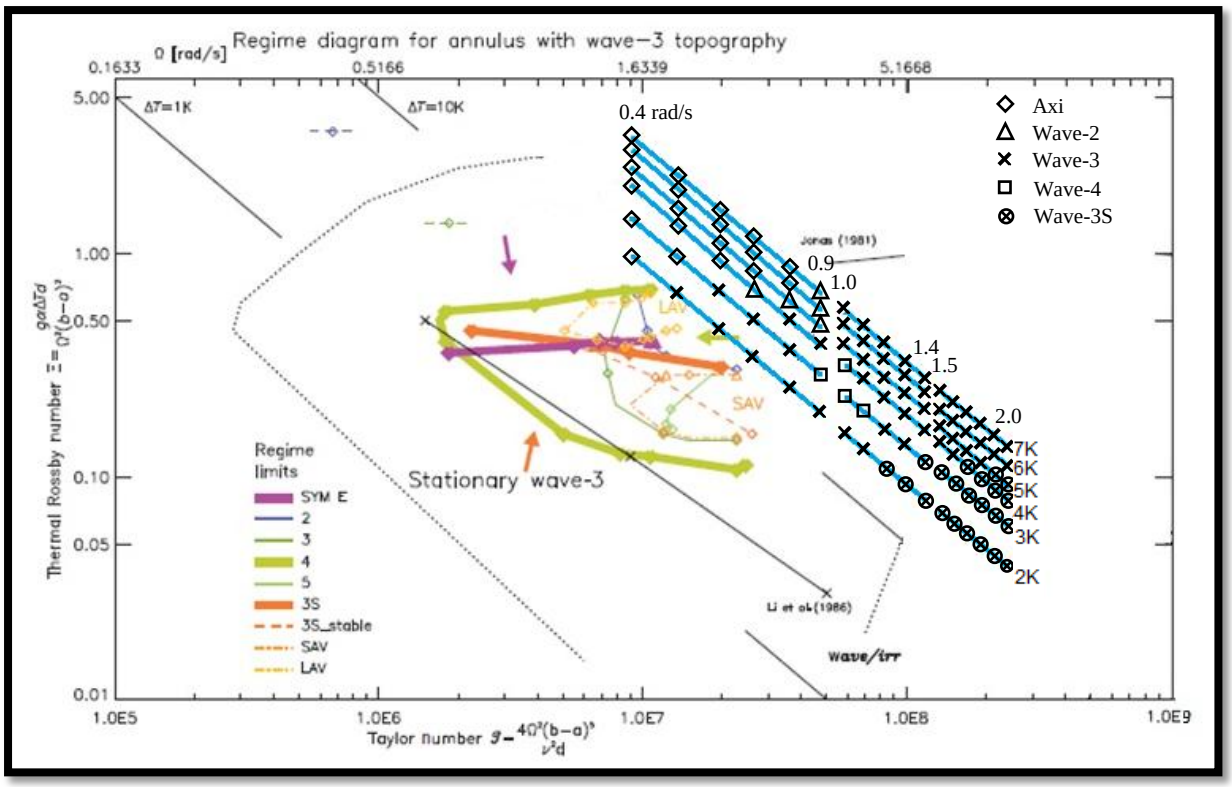

Figure 4.1: Extended regime diagram adapted from Read and Risch (2011), with locations and dominant flow characteristics of the results of the control experiment. All flows are drifting except for the stationary 'Wave-3S' region. Each point along the scans is 0.1 rads^{-1} apart.

Figure 4.1 shows that the flow types are confined to well-defined regions. The circulation starts off as axisymmetric, gaining a drifting wave structure as rotation rate increases, with possible transitions between wavenumber-2, wavenumber-3 and wavenumber-4 along the way. It can be noted, however, that wavenumber-3 is by far the most common. As the rotation rate increases even higher, the flow eventually becomes locked to a stationary wavenumber-3 type. To further illustrate these regions, an example of each flow structure is given below.

Axisymmetric

a.) **b.)** **c.)**

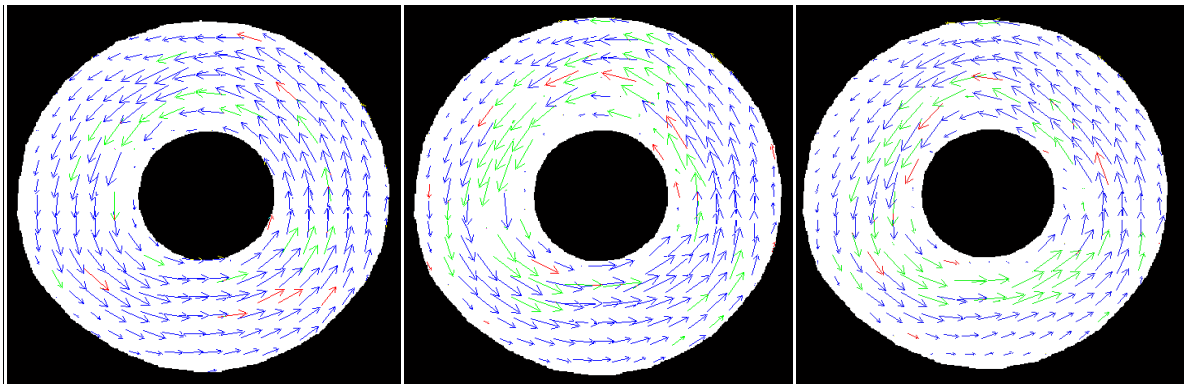

Figure 4.2: $\Omega = 0.4\ rads^{-1}$, $\Delta T = 2K$, $\mathcal{T} = 9.088x10^{6}$, $\theta = 0.988$, *a.)* $t = 3600s$, *b.)* $t = 5400s$, *c.)* $t = 7200s$

Figure 4.2 gives an example of axisymmetric flow. It can be noticed that the flow is slightly irregular, especially in (c), where hints of a weak wavenumber-3 flow can be observed. This effect is fleeting, however, and the dominant characteristics are of axisymmetric structure. In these diagrams blue vectors are those with the best correlation, green vectors denote reasonable correlation whilst red vectors have poor correlation. Any vector with less correlation than red has been removed.

Drifting Waves

a.) **b.)** **c.)**

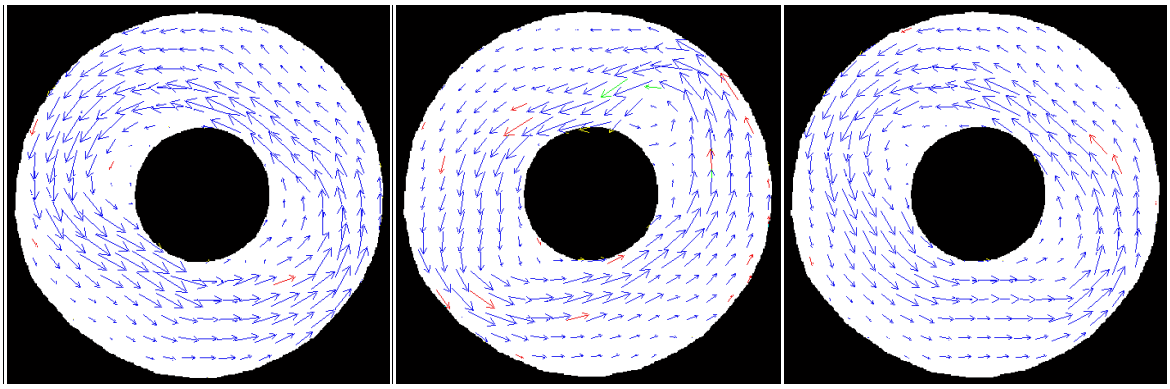

Figure 4.3: $\Omega = 0.7\ rads^{-1}$, $\Delta T = 4K$, $\mathcal{T} = 2.783x10^{7}$, $\theta = 0.645$, *a.)* $t = 3600s$, *b.)* $t = 5400s$, *c.)* $t = 7200s$

a.) **b.)** **c.)**

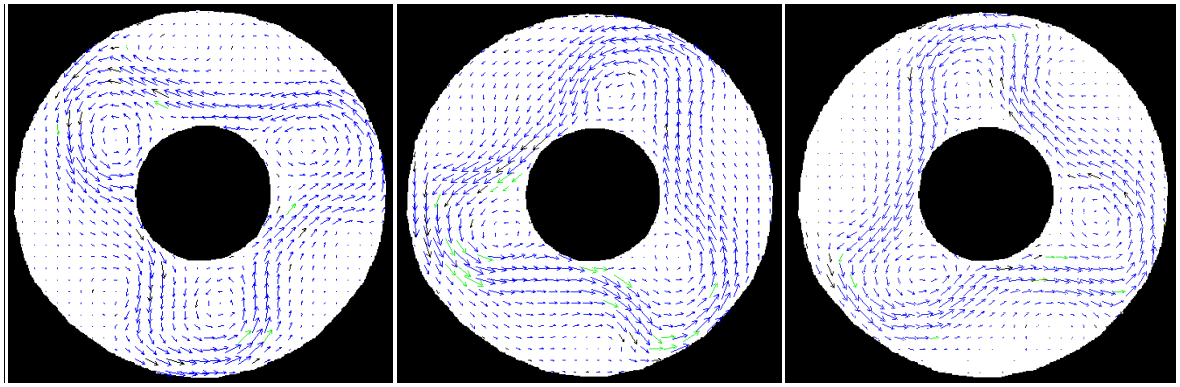

Figure 4.4: $\Omega = 0.6\ rads^{-1}$, $\Delta T = 2K$, $\mathcal{T} = 2.045x10^7$, $\theta = 0.439$, *a.)* $t = 3600s$, *b.)* $t = 5400s$, *c.)* $t = 7200s$

a.) **b.)** **c.)**

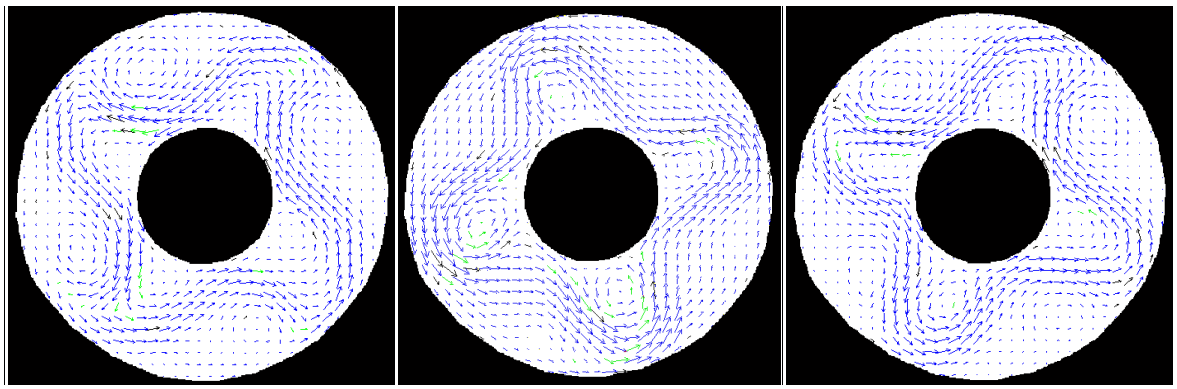

Figure 4.5: $\Omega = 1\ rads^{-1}$, $\Delta T = 3K$, $\mathcal{T} = 5.680x10^7$, $\theta = 0.237$, *a.)* $t = 3600s$, *b.)* $t = 5400s$, *c.)* $t = 7200s$

The above Figures are examples of flows that continually drift counter-clockwise (i.e. downstream). As discussed in Figure 4.1, the most common drifting flow is a wavenumber-3, shown in Figure 4.4. This is likely to be due to the locking effect of the topography. In additional, whilst wavenumber-3 can occur seemingly anywhere within the drifting region, the number of waves present does appear to be linked to the value of the Rossby Number. A high value near to the axisymmetric regime (such as in Figure 4.3) gives more wavenumber-2 flows, whilst a lower number (such as in Figure 4.5) are more likely to produce wavenumber-4 structures. An even lower Rossby Number once again returns to a domination of wavenumber-3, as the circulation prepares to enter the stationary wavenumber-3 regime.

Stationary Waves

a.) **b.)** **c.)**

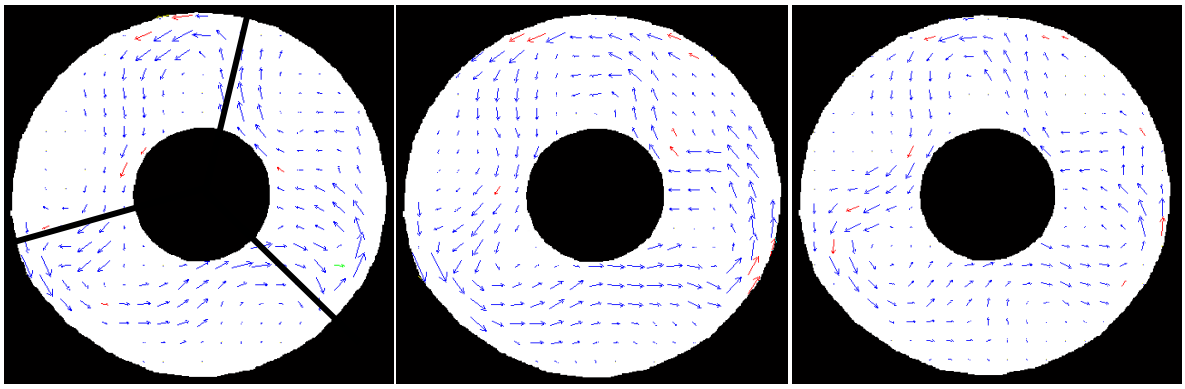

Figure 4.6: $\Omega = 1.2\ rads^{-1}$, $\Delta T = 2K$, $\mathcal{T} = 8.179x10^{7}$, $\theta = 0.110$, *a.)* $t = 3600s$, *b.)* $t = 5400s$, *c.)* $t = 7200s$

Figure 4.6 provides an example of a stationary wavenumber-3 flow structure. It can be observed that, whilst the waves do not move location, their shape changes noticeably over time. This is especially clear for the bottom-left wave and is likely evidence for structural vacillation at this point in parameter space. An indication of where the peaks of the topography lie has been added to (a). From this it can be seen that the waves occur slightly downstream from the corresponding wavenumber-3 shape of the topography, indicating a small phase-shift.

4.1.1 Vacillation

After the above readings had been carried out, the difficulties with the Mac Mini began. As such, the data acquisition method switched to using the replacement webcam and creating streakline images by finding and summing the differences between individual frames in MATLAB. The webcam has a frame-rate of 16.5 frames/second and it was found that the optimal images were made via 6 captures with a 15 frame interval between each, giving effective streaks of roughly 6.6 seconds. Hence the images show where the particles have travelled in the last 6.6 seconds - long streaks denote a quickly travelling particle, whilst shorter streaks and dots denote slower particles. As these readings are taken in realtime, slowly developing flow characteristics, such as vacillation, can be more easily observed. Once again, the regime diagram of Figure 4.11 will be updated with the new vacillation information at each point.

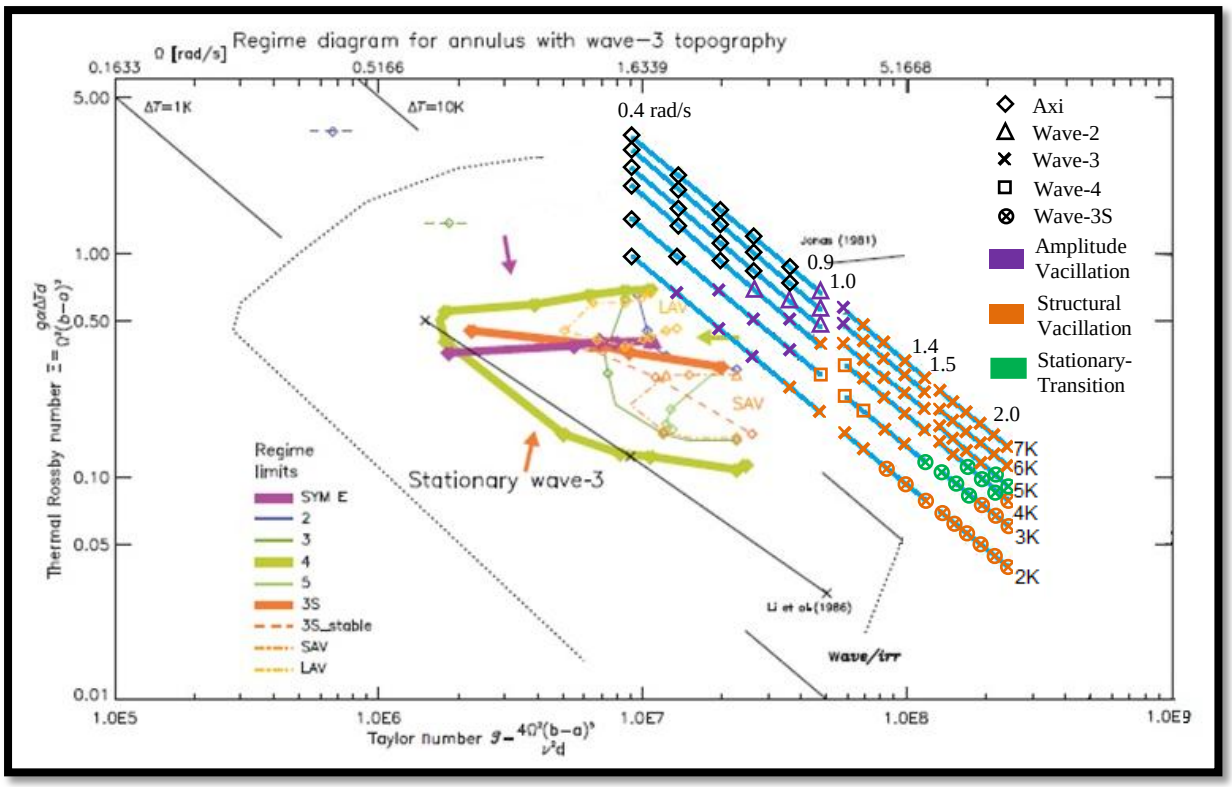

Figure 4.7: Extended regime diagram adapted from Read and Risch (2011); same as Figure 4.1 but with additional vacillation information.

Like the flow structures discussed in Figure 4.1, Figure 4.7 shows that the vacillation types also occur in well-defined regions. As soon as the flow changes from axisymmetric to drifting, amplitude vacillation (purple) can be observed. Similarly, as rotation rate increases further, this gives way to structural vacillation (orange), which continues for the rest of the readings. Within the structural vacillation region, another regime was discovered. This 'stationary-transition' regime (green) also undergoes structural vacillation, but is notable for its irregular oscillation between drifting and stationary waves. Once again, to further illustrate these regions, an example of each flow structure is given below.

Amplitude Vacillation

a.) **b.)**

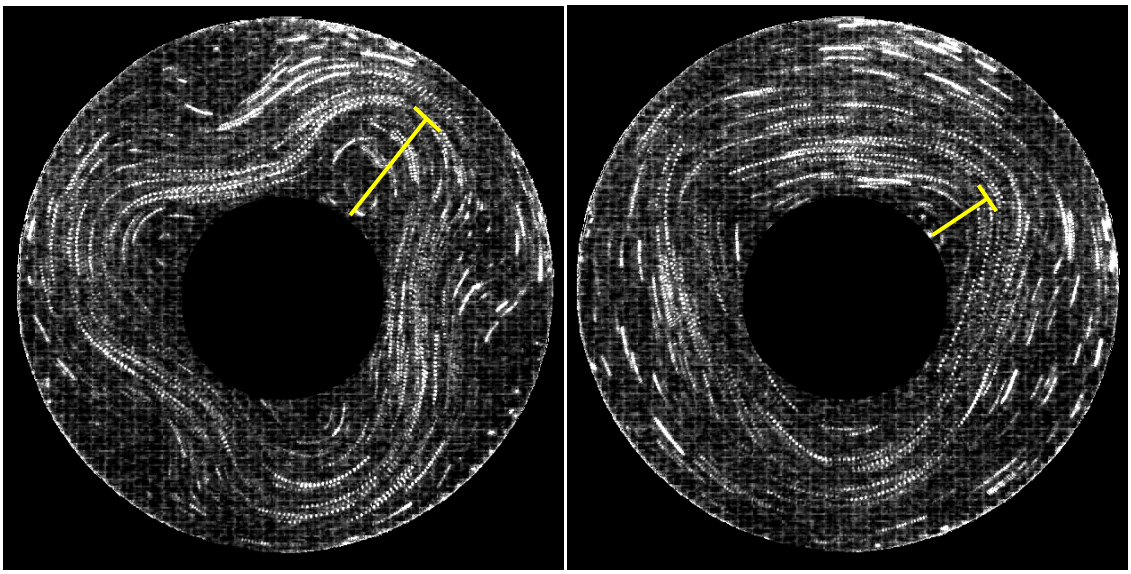

Figure 4.8: $\Omega = 0.6\ rads^{-1}$, $\Delta T = 2K$, $\mathcal{T} = 2.045x10^{7}$, $\theta = 0.439$, *a.)* $t = 4140s$, *b.)* $t = 4260s$

Lu and Miller (1998) characterise amplitude vacillation as a periodic oscillation of growth and decay of wave amplitude. To demonstrate this, the two images in Figure 4.8 show the maximum (a) and minimum (b) amplitude of a wavenumber-3 structure as it drifts downstream. The oscillation is regular, with a period of about 240 seconds. Deciding that the midpoint of the wave in (a) is the length of the yellow bar; the maximum amplitude is roughly 7.6 cm. Making the same assumption for (b) gives the minimum amplitude as roughly 4 cm.

Structural Vacillation

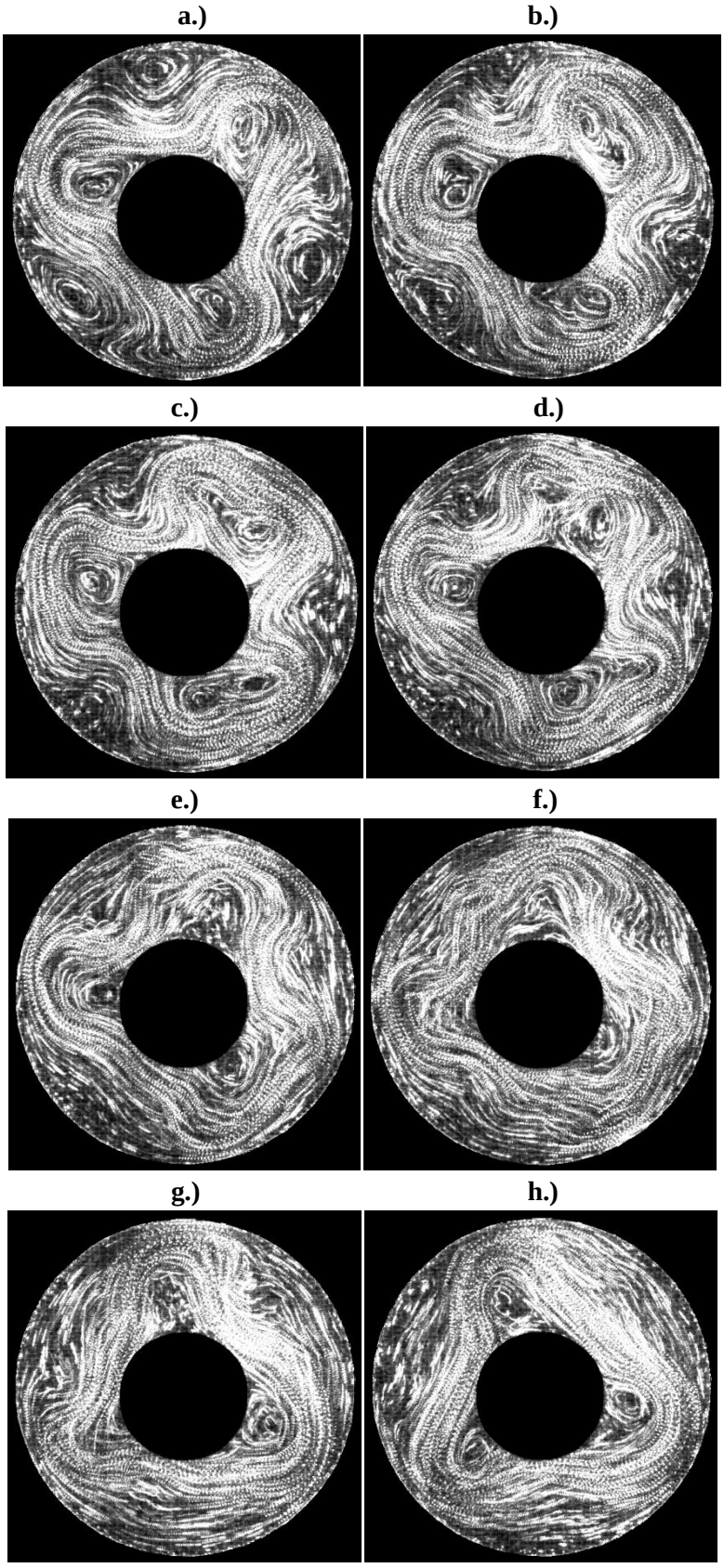

Figure 4.9: $\Omega = 1.4\ rads^{-1}$, $\Delta T = 7K$, $\mathcal{T} = 1.113x10^{8}$, $\theta = 0.282$, *a.)* $t = 4920s$, *b.)* $t = 4940s$, *c.)* $t = 4960s$, *d.)* $t = 4980s$, *e.)* $t = 5000s$, *f.)* $t = 5020s$, *g.)* $t = 5040s$, *h.)* $t = 5060s$

Figure 4.9 provides an image sequence illustrating one example of structural vacillation, defined in Read et al (2004) as "irregular, small-scale secondary instabilities or eddies" that affect the main flow pattern. The drifting flow in (a) starts off as a regular wavenumber-3 structure, but then begins to deform over time: (b) and (c) show the shape of the waves dramatically change; (d) and (e) show 'wave-nodes' appearing and eddies breaking off from the main waves in the downstream direction; (f) and (g) show the locations of the waves change relative to each other, forming a straighter jet along the bottom of the images. In (h), 140 seconds after the first image, the flow has returned to a regular wavenumber-3 structure. This oscillation is not as regular as the equivalent one from amplitude vacillation, and has no clear progression in terms of how the structure will deform during the vacillation.

Stationary-Transition

Of particular note in Figure 4.7 is the section outlined in green. This was observed to be some manner of 'stationary-transition' region where the flow was dominated by a stationary wavenumber-3 flow, but would occasionally lapse into a drifting flow or a chaotic structure (depending on the magnitude of the input parameters), and then return to the locked state. In the chaotic lapses, the flow appears to suffer from strong structural vacillation before eddies break off the wavenumber-3 structure and drift downstream. No illustration is given, as most of the time the flow structure is as in Figure 4.6, with lapses resembling Figure 4.4 or the chaotic portion of Figure 4.9.

4.2 Analysis – Control Experiment

From Figure 4.7, an easy comparison can be made between the results of the control experiment and those of Read and Risch (2011). This comparison shows that the flow structures and vacillation types occur almost exactly where expected if the green 'anvil' were to be extrapolated, tending to occur roughly across lines of constant Rossby Number. The axisymmetric regime is above the 'anvil', the drifting waves (wavenumbers-2,-3 and -4, as predicted) lie within the 'anvil' and stationary wavenumber-3 flows appear beneath the 'anvil'. Similarly, amplitude and structural vacillation were found across from the regions in which they were noted by Read and Risch, provided that the structural vacillation region is assumed to expand as Taylor Number increases, to the extent that it starts occurring outside of the 'anvil' and in the stationary regime as well. This expansion would also explain why Read and Risch found areas with no vacillation, but the control experiment did not. In addition, the large spread of structural vacillation would account for the relatively common occurrence of atypical wave structures and additional 'wave lobes', especially in regions of high rotation rate and temperature difference, where structural vacillation increases in intensity.

The results gathered also agree well with established topographic theory. As discussed in Chapters 1 and 2, the most notable effect of the addition of topography is the formation of stationary topographic waves, locked at locations determined by the shape and position of the base. This is the spatial symmetry-breaking effect on the zonal flow mentioned by Benzi et al (1986). The small phase shift noticed in the stationary waves of Figure 4.6 can be explained by the fact that, in the Northern Hemisphere, topographic waves slope westward (i.e. downstream) with height[10]. This phase-shift has also been observed in other annuli experiments, such as those of Leach (1981).

The most unexpected discovery of the control experiment was the 'stationary-transition' region, found whilst searching for vacillations. This region is thought to occur due to the strong rotational and thermal forcing acting upon the circulation being able to temporarily interrupt the weak locking of the topography, possibly as a side-effect of the structural vacillation present. For reference, the region occurs at a point in parameter space where, were there no topography, chaotic flow would be expected[11]. However, as the rotation rate is increased further (roughly until the Rossby Number drops to 0.079), the locking of the topography becomes stronger and the stationary structure no longer breaks down.

4.3 Partial Barrier Experiment

As these readings were to be taken with the substitute webcam and not the permanent replacement, they were to be considered just preliminary results. As such, like in the previous study, only a single lighting layer was employed.

Unfortunately, at this time, no viable readings have been made from the partial barrier experiments. This was due to a new and unforeseen problem: during the readings, the heating element of the outer cylinder started malfunctioning, making maintaining a constant temperature difference impossible. Whilst this issue is currently in the process of being fixed, the corresponding delay has prevented the acquisition of preliminary results. The experiments are expected to be resumed by the submission date of this report.

[10] Noted by Reinhold and Pierrehumbert (1982), amongst others.
[11] As found in the first year of this project.

Chapter 5

Preliminary Conclusions

In this chapter the various results and observations of Chapter 4 will be examined in greater detail, with a discussion on what has been learnt from the studies so far. A final section will then highlight the outstanding issues of the second-year experiments, both in terms of possible methods to improve the results gathered and further extensions to the studies to investigate other aspects of topographic impact of the flow.

5.1 Discussion – Control Experiment

The most important objective of the control experiment was to explore a large, varied area of parameter space in order to create a basis for comparison for all future experiments. In this way the control experiment has been very successful. As discussed in the previous chapter, the investigation found what was expected to be found, both in terms of a continuation of the readings of Read and Risch (2011), and comparison with the effects of topography given in the literature. In addition, Figure 4.7 provides a sizable number of different flows in terms of characteristics and regimes. The experiments with other topographies will be able to contrast which regimes are encountered, and where they occur in parameter space. In particular, the size and location of the unexpected 'stationary-transition' region will be thoroughly investigated in each study.

As a secondary finding, the MATLAB code written to generate streakline images was found to produce good quality readings of particle motion. The realtime updating feature also allowed simple observation of flow characteristics with longer time-scales, such as vacillation (Figures 4.8 and 4.9). The visualisation software used is therefore clearly viable for results gathering in the subsequent years of this thesis. When the permanent replacement for the Mac Mini is installed, the experiments will be able to employ both these streakline images for quick flow characterisation, and the vector velocity diagrams from CIV for more in-depth model analysis, such as delay coordinate reconstructions.

The foremost weakness of the study so far was that the preliminary partial barrier experiments could not be completed on time due to equipment failure. As such, no comparison could yet be made between the different topographies. Furthermore, because the only finished investigation was a control, few original results can be presented.

5.3 Outstanding Issues

The most obvious way to extend the current studies further would be to take more readings at different temperature differences or rotation rates. The best use of this expansion would be to gain data at higher rotation rates than 2 $rads^{-1}$, as this would allow the lower limit of the stationary wavenumber-3 regime to be observed, possibly illustrating a route to chaos. In addition, more information on the 'stationary-transition' region could also be obtained. The main reason this is not being carried out in the current studies is that more scans would mean too much time being spent on each individual experiment, slowing down the investigation as a whole. Similarly, in order to account for hysteresis, scans of decreasing rotation rate or runs set to a specific point in parameter space could also be employed. However, results from the first year of this project suggest that hysteresis has a relatively low effect under these conditions.

In the beginning of the partial barrier experiment it was noticed that the illumination from the lighting array was weak at levels other than the one chosen for the control experiment. Improvements will have to be made before proper baroclinic data can be acquired. Poor visualisation results were also caused by sinking tracer particles – this can solved by using a denser working fluid (i.e. a mixture weighted slightly more toward glycerol) and adding more particles in suspension.

Chapter 6

Further Work and Timeline

This chapter will summarise all the tasks planned for the future of this thesis. Firstly, the current plan for the replacement of the Mac Mini will be described, along with other possible improvements to the equipment. After that, a planned numerical study to complement the laboratory work will be discussed and its importance explained. Finally, a timeline is provided to illustrate when all of these tasks are planned to take place in the course of the thesis.

6.1 Experimental Improvement

The original Firewire camera boasted loss-less data compression and could achieve higher resolution images than the webcam replacement. As such, it is planned that the Firewire camera will remain the principal device for visual data acquisition. The Mac Mini, on the other hand, was not perfected suited for its task (due to low RAM and hard-drive space, for example), so instead of a new one, a Small Form Factor PC with Firewire capabilities is being looked into. Other than this change to a Windows OS, the hardware and software should remain mostly the same.

During the time needed for the new computer to be installed, other improvements to the apparatus can be added. Whilst the various leaks of the heating and cooling systems had no practical impact on the investigation, and therefore could safely be ignored, the lighting array was found to be far more problematic. At some point prior to the beginning of this thesis the metal of the array had seemingly deformed, causing the lights to no longer exactly align with their respective slits in the annulus. As such, the illumination is below optimal, especially at lower levels. Whilst this issue could be fixed, it seems prudent to replace the array of lamps with one of Ultra-Bright LEDs. Not only would this fix the illumination problem, but the light would be more focussed and less susceptible to picking up particles outside of its level. In addition, the three electric fans could be removed, reducing weight and clutter on the rotating frame.

Once the rig is fully operational again and improvements complete, the partial barrier experiments can resume with both the vector velocity diagrams via Coriolis, and the streakline images via MATLAB. The code for the latter will be optimised for the Firewire camera, and should be able to produce a superior quality than the results from the webcam. The topographic investigation will then proceed as described in Figure 3.13.

6.2 Numerical Study

QUAGMIRE, standing for *QUAsi-Geostrophic Model for Investigating Rotating fluids Experiments*, is different to those numerical models most commonly used in the literature (as mentioned in Chapter 2), as it is not employed to search for new atmospheric phenomena, but instead to increase the understanding of those already found. As the name suggests, it attempts to achieve this by having geometry in the form of a rotating annulus like those used in laboratory. Unlike the otherwise similar MORALS (*Met Office/Oxford Rotating Annulus Laboratory Simulation*, see Farnell and Plumb (1975) for a full description), instead of attempting the full Navier-Strokes Equations and the many other equations that describe a flow, QUAGMIRE only solves the quasi-geostrophic potential vorticity equation. Williams, Read and Haine (2010) explained that, due to their simplicity and thus their ease of modelling, laboratory flows are excellent for studying "fundamental dynamical phenomena". However, the authors believed that models that solve the Navier-Strokes Equations are too computationally expensive to use for a large enough sample of flows. QUAGMIRE is the solution to this problem, with its greatly reduced computational expense. The model is also multi-layer, allowing the vertical structure of the atmosphere to be investigated as rigorously or as roughly as required[12]. On the other hand, the use of the quasi-geostrophic approximation means that no ageostrophic features of the flow can be simulated. The most notable absences are the boundary layers, which in turn mean no Ekman Layers can exist. The remedy for this is to set boundary conditions via Ekman Pumping, but ageostrophic features will still not be modelled.

The reasoning behind using QUAGMIRE is twofold: firstly, as Hignett et al (1985) noted, an additional numerical study can greatly improve the accuracy of a laboratory study. The numerical model QUAGMIRE, already set up to simulate a differentially-heated annulus, will be employed for the same topographies, allowing comparison between the experimental and computational studies. The results gathered from these experiments will be contrasted, highlighting and removing as many errors as possible and hence reducing the risk of nonsense readings from either source.

[12] One- and two-layer models have already been discussed and, for example, Kondrashov, Ide and Ghil (2004) achieved a 'realistic' global simulation using a three-layer model.

Secondly, and most importantly, QUAGMIRE is a quasi-geostrophic model. Comparing its results to those from the physical annulus will test the limits of quasi-geostrophic theory. The theory is known to begin to break down at roughly the point where the ratio of the height of the topography to the height of the annulus becomes greater than or equal to the Rossby Number of the flow. This is what occurs in the atmosphere, if the height of the annulus is replaced by the height of the tropopause. As such, the magnitude of the topography designed, as well as the flow parameters used, were chosen in such a way that this condition is met. The comparisons between the experiments will therefore show how well a quasi-geostrophic model copes in an ageostrophic environment and which ageostrophic aspects of sloping convection, if any, can be imitated. In addition, any flow features observed in the laboratory study, but not the numerical study, can be assumed to be ageostrophic in nature.

6.3 Timetable

Figure 6.1 shows an estimated timeline of this project, running from the current time until its end in the summer of 2012. The length of time allotted to each task is intentionally generous, to take into account the various potential delays for those assignments (such as long delivery times for parts). Hopefully, this will also mitigate the effect of any unforeseeable problems encountered (such as equipment failure or illness). As topography is the main focus of the second and third year of this thesis, possible studies into other phenomena (such as bifurcations and inertia-gravity waves, investigated in the first year) will not be explicitly factored into the planned timeline. The penultimate task, however, is amongst the longest, allowing ample scope for further studies and experiments to be carried out, if the project does not fall behind schedule.

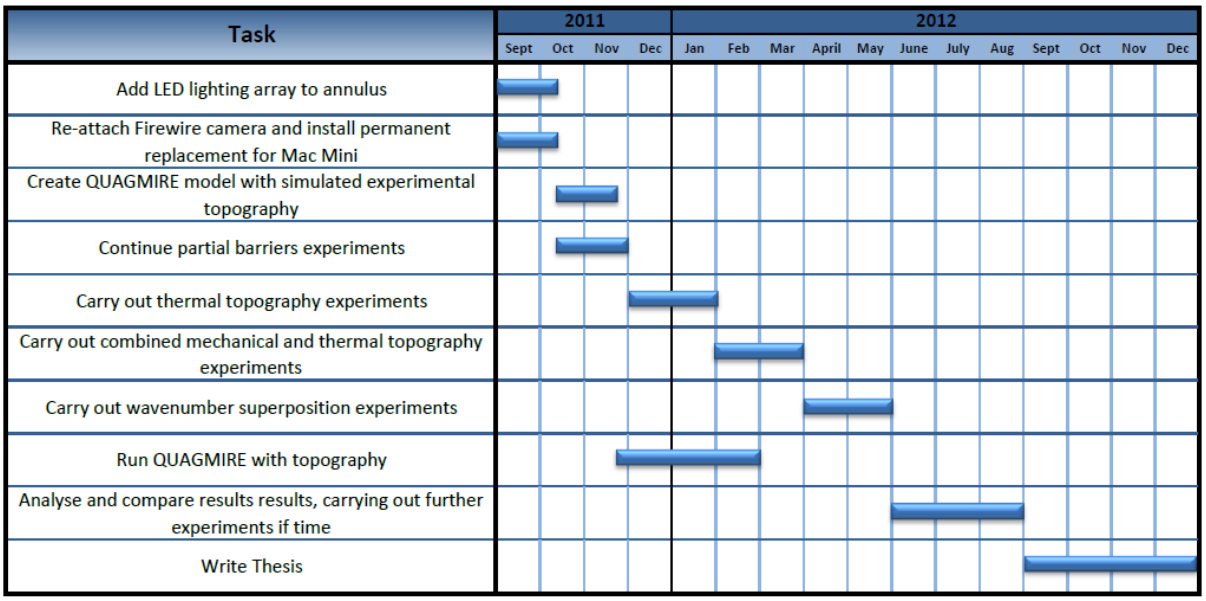

Figure 6.1: Proposed timeline for thesis

References

Allen, J.S., 1980. Models of Wind-Driven Currents on the Continental Shelf. *Ann. Rev. Fluid Mech.*, **12**, pp. 389-433.

Allen, J.S. & Newberger P.A., 1996. Downwelling Circulation on the Oregon Continental Shelf, Part I: Response to Idealized Forcing. *J. Phys. Oceanogr.*, 26(10), pp. 2011-2035.

Andrews, D.G., 2000. *An Introduction to Atmospheric Physics*. Cambridge: Cambridge University Press.

Benzi, R., Malguzzi, P., Speranza, A. & Sutera, A., 1986. The Statistical Properties of General Atmospheric Circulation: Observational Evidence and a Minimal Theory of Bimodality. *Quarterly Journal of the Royal Meteorological Society*, 112(473), pp.661-674.

Berggren, R., Bolin, B. & Rossby, C-G., 1949. An Aerological Study of Zonal Motion, its Perturbations and Break-down. *Tellus*, 1(2), pp. 14-37.

Bernardet, P., Butet, A., Déqué, M., Ghil, M. & Pfeffer, R.L, 1990. Low Frequency Oscillations in a Rotating Annulus with Topography. *J. Atmos. Sci.*, 47(24), pp.3023-3043.

Boubnov, B.M., Golitsyn, G.S. & Senatorsky, A.O., 1991. Convection in a Rotating Cylindrical Annulus with Azimuthally Non-Uniform Heating. *Geophys. Astrophys. Fluid Dyn.*, 57(1), pp. 1-18.

Boyer, D.L. & Chen. R., 1987. Laboratory Simulations of Mechanical Effects of Mountains on the General Circulation of the Northern Hemisphere: Uniform Shear Background Flow. *J. Atmos. Sci.*, 44(23), pp.3552-3575.

Cehelsky, P. & Tung, K.K., 1987. Theories of Multiple Equilibria and Weather Regimes – A Critical Reexamination. Part II: Baroclinic Two-Layer Models. *J. Atmos. Sci.*, 44(21), pp.3282-3303.

Charney, J.G. & DeVore, J.G., 1979. Multiple Flow Equilibria in the Atmosphere and Blocking. *J. Atmos. Sci.*, 36(7), pp.1205-1216.

Charney, J.G. & Straus, D.M., 1980. Form-Drag Instability, Multiple Equilibria and Propagating Planetary Waves in Baroclinic, Orographically Forced, Planetary Wave Systems. *J. Atmos. Sci.*, 37(6), pp.1157-1176.

Charney, J.G., Shukla, J. & Mo, K.C., 1981. Comparison of a Barotropic Blocking Theory with Observation. *J. Atmos. Sci.*, 38(4), pp.762-779.

Farnell, L. & Plumb, R.A., 1975. Numerical Integration of Flow in a Rotating Annulus I: Axisymmetric Model. *Occasional Note Met O*, 21 75/3. [Unpublished Technical Report]

Federiuk, J. & Allen, J.S., 1995. Upwelling Circulation on the Oregon Continental Shelf, Part II: Simulations and Comparisons with Observations. *J. Phys. Oceanogr.*, 25(8), pp. 1867-1889.

Fowlis, W.W. & Hide, R., 1965. Thermal Convection in a Rotating Annulus of Liquid: Effect of Viscosity on the Transition between Axisymmetric and Non-Axisymmetric Flow Regimes. *J. Atmos. Sci.*, **22**, pp. 541-558.

Ghil, M. & Robertson, A.W., 2002. "Waves" vs. "Particles" in the Atmosphere's Phase Space: A Pathway to Long-Range Forecasting? *Proceedings of the National Academy of Sciences of the United States of America*, 99(1), pp.2493-2500.

Held, I.M., 1983. Stationary and Quasi-Stationary Eddies in the Extratropical Troposphere: Theory. In Hoskins, B.J. & Pearce, R.P., ed., *Large-Scale Dynamical Processes in the Atmosphere*. London: Academic Press Inc. (London) Ltd. Ch. 6.

Hide, R., 1953. Some Experiments on Thermal Convection in a Rotating Liquid. *Quarterly Journal of the Royal Meteorological Society*, 79(339), pp.161. [Correspondence]

Hide, R., 1958. An Experimental Study of Thermal Convection in a Rotating Liquid. *Philosophical Transactions of the Royal Society of London. Series A, Mathematical and Physical Sciences*, 250(983), pp.441-478.

Hide, R., Lewis, S.R. & Read, P.L., 1994. Sloping Convection: A Paradigm for Large-Scale Waves and Eddies in Planetary Atmospheres? *Chaos*, 4(2), pp.135-162.

Hide, R. & Mason, P.J., 1975. Sloping Convection in a Rotating Fluid. *Advances in Physics*, 24(1), pp.47-100.

Hignett, P., White, A.A., Carter, R.D., Jackson, W.D.N. & Small, R.M., 1985. A Comparison of Laboratory Measurements and Numerical Simulations of Baroclinic Wave Flows in a Rotating Cylindrical Annulus. *Quarterly Journal of the Royal Meteorological Society*, 111(463), pp.131-154.

Hollingsworth, J.L. & Barnes, J.R., 1996. Forced Stationary Planetary Waves in Mars's Winter Atmosphere. *J. Atmos. Sci.*, 53(3), pp.428-448.

Holton, J.R., 1992. *An Introduction to Dynamic Meteorology*. 3rd ed. New York: Academic Press.

Houghton, J., 2002. *The Physics of Atmospheres*. 3rd ed. Cambridge: Cambridge University Press.

Huthnance, J.M., 1989. Internal Tides and Waves near the Continental Shelf Edge. *Geophys. Astrophys. Fluid Dyn.*, 48(1-3), pp. 81-106.

James, I.N., 1988. Meteorology of a Flat Earth. *Nature*, **333**, pp.118.

Jonas, P.R., 1981. Laboratory Observations of the Effects of Topography on Baroclinic Instability. *Quarterly Journal of the Royal Meteorological Society*, 107(454), pp.775-792.

Kaspi, Y. & Schneider, T., 2011. Winter Cold of Eastern Continental Boundaries Induced by Warm Ocean Waters. *Nature*, **471**, pp. 621–624.

Keppenne, C.L., 1992. Orographically Forced Oscillations in a Dynamical Model of the Martian Atmosphere. *Icarus*, 100(2), pp.598-607.

Keppenne, C.L. & Ingersoll, A.P., 1995. High-Frequency Orographically Forced Variability in a Single-Layer Model of the Martian Atmosphere. *J. Atmos. Sci.*, 52(11), pp.1949-1958.

Kondrashov, D., Ide, K. & Ghil, M., 2004. Weather Regimes and Preferred Transition Paths in a Three-Layer Quasigeostrophic Model. *J. Atmos. Sci.*, 61(5), pp.568-587.

Koo, S. & Ghil, M., 2002. Successive Bifurcations in a Simple Model of Atmospheric Zonal-Flow Vacillation. *Chaos*, 12(2), pp.300-309.

Leach, H., 1981. Thermal Convection in a Rotating Fluid: Effects due to Bottom Topography. *J. Fluid Mech.*, **109**, pp.75-87.

Li, Q.G., Kung, R. & Pfeffer, R.L., 1986. An Experimental Study of Baroclinic Flows with and without Two-Wave Bottom Topography. *J. Atmos. Sci.*, 43(22), pp.2585-2599.

Lu, H-L. & Miller, T.L., 1998. Characteristics of Annulus Baroclinic Flow Structure During Amplitude Vacillation. *Dyn. Atmos. Oceans*, 27(1-4), pp. 485-503.

Luo, D., 2005. A Barotropic Envelope Rossby Soliton Model for Block–Eddy Interaction, Part I: Effect of Topography. *J. Atmos. Sci.*, **62**, pp. 5–21.

Molteni, F., 1996. On the Dynamics of Planetary Flow Regimes, Part II: Results from a Hierarchy of Orographically Forced Models. *J. Atmos. Sci.*, 53(14), pp.1972-1992.

Nayvelt, L., Gierasch, P.J. & Cook, K.H., 1997. Modeling and Observations of Martian Stationary Waves. *J. Atmos. Sci.*, 54(8), pp. 986-1013.

Rayer, Q.G., Johnson, D.W. & Hide, R., 1998. Thermal Convection in a Rotating Fluid Annulus Blocked by a Radial Barrier. *Geophys. Astrophys. Fluid Dyn.*, 87(3), pp. 215-252.

Read, P.L. & Lewis, S.R., 2004. *The Martian Atmosphere Revisited: Atmosphere and Environment of a Desert Planet*. Chichester: Praxis Publishing Ltd.

Read, P.L., Maubert, P., Randriamampianina, A. & Früh W-G., 2004. DNS of Transitions towards Structural Vacillation in an Air-Filled, Rotating Baroclinic Annulus, *J. Fluid Mech.*, [Submitted]

Read, P.L. & Risch, S.H., 2011. A Laboratory Study of Global-Scale Wave Interactions in Baroclinic Flow with Topography, Part I: Multiple Flow Regimes. *Geophys. Astrophys. Fluid Dyn.*, 105(2-3), pp. 128-160.

Reinhold, B.B. & Pierrehumbert, R.T., 1982. Dynamics of Weather Regimes: Quasi-Stationary Waves and Blocking. *Mon. Wea. Rev.*, 110(9), pp.1105-1145.

Risch, S.H., 1999. *Large-Scale Wave Interactions in Baroclinic Flow with Topography*. DPhil. University of Oxford.

Tian, Y., Weeks, E.R., Ide, K., Urbach, J.S., Baroud, C.N., Ghil, M. & Swinney, H.L., 2001. Experimental and Numerical Studies of an Eastward Jet over Topography. *J. Fluid Mech.*, **438**, pp.129-157.

Tung, K.K. & Rosenthal, A.J., 1985. Theories of Multiple Equilibria and Weather Regimes – A Critical Reexamination. Part I: Barotropic Models. *J. Atmos. Sci.*, 42(24), pp.2804-2819.

Vettin, F., 1857. Ueber den aufsteigenden luftstrom, die entstehung des hagels und der wirbel-stuerme. *Annalen der Physik*, 178(10), pp.246-255.

Völker, C., 1999. Momentum Balance in Zonal Flows and Resonance of Baroclinic Rossby Waves. *J. Phys. Oceanogr.*, 29(8), pp.1666-1681.

Wallace, J.M., 1983. The Climatological Mean Stationary Waves: Observational Evidence. In Hoskins, B.J. & Pearce, R.P., ed., *Large-Scale Dynamical Processes in the Atmosphere*. London: Academic Press Inc. (London) Ltd. Ch. 2.

Williams, P.D., Read, P.L. & Haine, T.W.N., 2010. Testing the Limits of Quasi-Geostrophic Theory: Application to Observed Laboratory Flows Outside of the Quasi-Geostrophic Regime. *J. Fluid Mech.*, **649**, pp.187-203.

Wordsworth, R.D., 2008. *Theoretical and Experimental Investigations of Turbulent Jet Formation in Planetary Fluid Dynamics.* DPhil. University of Oxford.

Yang, S., Reinhold, B. & Källén, E., 1997. Multiple Weather Regimes and Baroclinically Forced Spherical Resonance. *J. Atmos. Sci.*, 54(11), pp.1397-1409.